

from human ES cells to EC or other vascular cell components, such as MC, in the embryoid body differentiation system has so far not been possible.

In the study reported here, we identified the differentiation kinetics of human ES cells to vascular cell components by using our *in vitro* 2D differentiation system. Furthermore, we succeeded in establishing new human cell sources derived from human ES cells, which may be used for therapeutically effective transplantation *in vivo*.

## Methods

### Cell Culture

ES cells were maintained as described.<sup>1,7</sup> OP9 feeder cell lines were established and maintained as described,<sup>8</sup> whereas their growth was inactivated by mitomycin C.

To induce differentiation, ES cells were dissociated into small colonies with the aid of 0.1% collagenase (Wako) and cultured on an OP9 feeder layer in a differentiation medium (minimal essential medium, GIBCO) supplemented with  $5 \times 10^{-5}$  M 2-mercaptoethanol with 10% FCS. Sorted cells were recultured on a collagen IV-coated dish in the differentiation medium with the addition of 10% FCS, VEGF (100 ng/mL; PeproTech EC Ltd), or platelet-derived growth factor (PDGF)-BB (10 ng/mL) (PeproTech EC Ltd).

### Flow Cytometry and Cell Sorting

Cells were detached by cell dissociation buffer (GIBCO) with or without collagenase and labeled with various fluorescence-conjugated monoclonal antibodies (please see <http://atvb.ahajournals.org>). Flow cytometry analysis and cell sorting were performed as described.<sup>2,4,8</sup>

### Immunohistochemistry

Cultured cells were stained with various monoclonal antibodies (please see <http://atvb.ahajournals.org>) as described.<sup>2,4</sup> The immunofluorescence photographs were taken with a confocal laser-scanning microscope (LSM5-Pascal, Carl Zeiss).

### Hindlimb Ischemia Model

Eight-week-old KSN/Slc and BALB/c Slc nude mice were purchased from SLC Japan. After anesthetization with pentobarbital (80 mg/kg IP), the right femoral vein was ligated. We injected  $5 \times 10^5$  cells in 100  $\mu$ L of PBS or 100  $\mu$ L of PBS only into the right femoral artery. Immediately after the cell injection, the right femoral artery was ligated and excised.<sup>9</sup> Experimental procedures were performed in accordance with Kyoto University standards for animal care. Hindlimb blood flow was measured with a laser Doppler perfusion image analyzer (Moor Instruments Ltd), as described.<sup>9</sup> Biotin-conjugated Griffonia simplicifolia lectin I-isolectin B<sub>4</sub> (Vector Laboratories) was injected into the portal vein 15 minutes before sacrifice. After fixation with 4% paraformaldehyde, the ischemic lower legs were embedded in optimal cutting temperature compound (Sakura Finetechnical Co Ltd) and frozen. Capillary numbers were examined by counting the number of capillaries stained with anti-human and/or mouse CD31 antibody. Ten random fields on 2 different sections ( $\approx 3$  mm apart) from each mouse were photographed and analyzed by National Institutes of Health imaging as described.<sup>9</sup> The vessel area and length were measured quantitatively with the Kurabo angiogenesis image analyzer (Kurabo).

### Teratoma Formation Study

We transplanted  $5 \times 10^5$  cells in 50  $\mu$ L of PBS under the dorsal back skin of SCID mice (CLEA Japan, Inc), which are commonly used for teratoma formation for human ES cells.<sup>1,7</sup> After 5 months, 1 cm<sup>2</sup> of the skin around the point of injection was harvested, and the excised tissue was serially sectioned (10  $\mu$ m) at 200- $\mu$ m intervals.

### Analysis of Angiogenic Factor mRNA Expression

Total cellular RNA was isolated from VPCs or ECs in the early differentiation stage (eECs) with RNeasy Mini kit (Qiagen KK). The mRNA expression was analyzed with the One-Step RNA PCR kit (TaKaRa). Primer pairs were purchased from R&D Systems Inc. PCRs were performed as manufacturers protocols.

### Measurement of Angiogenic Factors in VPC- or eEC-Conditioned Media

Cells ( $1 \times 10^6$ ) of VPCs or eECs were plated on 10-cm dishes and incubated with 5 mL of media (minimal essential medium with 0.5% bovine serum) for 72 hours. The concentrations of human VEGF, basic fibroblast growth factor (bFGF), and hepatocyte growth factor (HGF) were measured by SRL, Inc. Human PDGF-BB was measured with the Human PDGF-BB Quantikine ELISA kit (R&D Systems Inc).

### Statistical Analysis

Results are presented as mean  $\pm$  SEM. In the hindlimb ischemia model, the statistical significance was evaluated using ANOVA followed by Fisher's analysis for comparisons between 2 means.  $P < 0.05$  was considered significant.

## Results

### Differentiation Pathway of Human ES Cells to Vascular Cell Components

First, we examined the expression of VEGF-R2 and some putative stem cell markers on a human ES cell line, HES3, which was established at Monash University in Australia.<sup>1</sup> Approximately 50% of undifferentiated human ES cells expressed VEGF-R2, whereas these cells were also positive for AC133 and c-Kit but negative for CD34, respectively (Figure 1A). We also analyzed the expression of tumor rejection antigen (TRA) 1-60 on these human ES cells. The TRA1 antigen is expressed on the surface of human tetracarcinoma stem cells, human embryonic germ cells, and human ES cells. Thus, we used it as a marker of the human ES cell. The VEGF-R2<sup>+</sup> population of human ES cells was also positive for TRA1-60 (Figure 1B).

Next, we induced differentiation of human ES cells in an *in vitro* 2D culture on an OP9 stromal cell line. Although monkey ES cells have effectively differentiated as single cells on an OP9 layer,<sup>10</sup> human ES cells have not survived as single cells. We, therefore, plated small human ES cell colonies on OP9 to induce differentiation. Under these conditions, the TRA1-60<sup>+</sup> cell population gradually decreased in number during differentiation. On the other hand, a VEGF-R2<sup>+</sup> TRA1-60<sup>-</sup> population emerged and accounted for  $\approx 15\%$  of all of the cells on day 8 (Figure 1C). We confirmed the differentiation kinetics of human ES cells by using another human ES cell line, KhES-1, established by us.<sup>7</sup> Similar to the HES3 cell line, VEGF-R2 was low positive, and the VEGF-R2<sup>+</sup> cells were also TRA1-60<sup>+</sup> in undifferentiated KhES-1 (Figure 1D). After differentiation on an OP9 feeder layer, VEGF-R2<sup>+</sup> TRA1-60<sup>+</sup> cells decreased, and VEGF-R2<sup>+</sup> TRA1-60<sup>-</sup> cells appeared on days 8 (Figure 1E). Next, we analyzed the expression of several cell surface markers on the VEGF-R2<sup>+</sup> TRA1-60<sup>-</sup> population on day 8 of HES3. Flt1 was positive, c-Kit and CXCR4 were both negative, PDGR receptor (PDGFR) $\alpha$  and PDGFR $\beta$  were positive, AC133

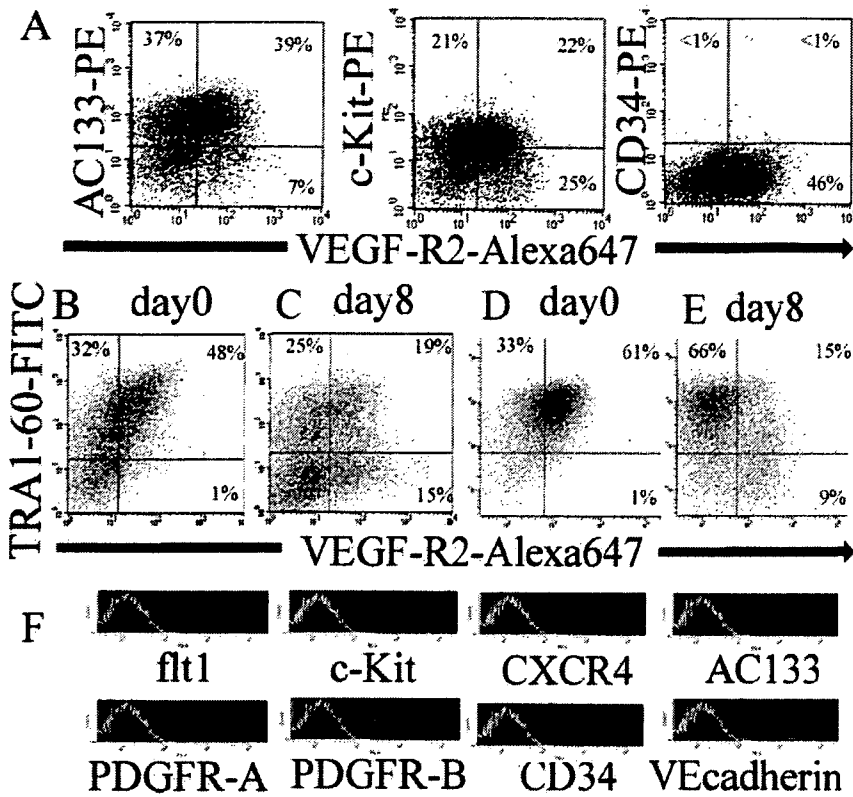


**Figure 1.** Flow cytometry analysis of differentiation kinetics of human ES cells. A, Expression of cell surface markers on undifferentiated human ES cells (HES3). B through E, TRA1-60 and VEGF-R2 expression on 2 human ES cell lines (HES3 and KhES-1) during differentiation on an OP9 feeder layer. B and C, HES3; D and E, KhES-1. F, Cell surface marker expression on VEGF-R2<sup>+</sup> TRA1-60<sup>-</sup> cells on day 8.

was still positive, and CD34 and vascular endothelial cadherin (VE-cadherin) were negative on a large population of the VEGF-R2<sup>+</sup> TRA1-60<sup>-</sup> cells (Figure 1F). Monocyte markers, such as CD45, Cd11b, and CD14, were negative.

The VEGF-R2<sup>+</sup> TRA1-60<sup>-</sup> and VE-cadherin-negative cells were sorted by flow cytometry on day 8 and cultured

on a collagen IV-coated dish without a feeder cell layer for an additional 8 days in the presence of 10% FCS and VEGF. This cell culturing condition induced the emergence of CD34<sup>+</sup>, VE-cadherin<sup>+</sup>, CD31<sup>+</sup>, and endothelial NO synthase-positive cells (Figure 2A through 2D), which can be categorized as ECs. The rest of the cells negative for CD31 were polygonal in shape and showed  $\alpha$ -smooth

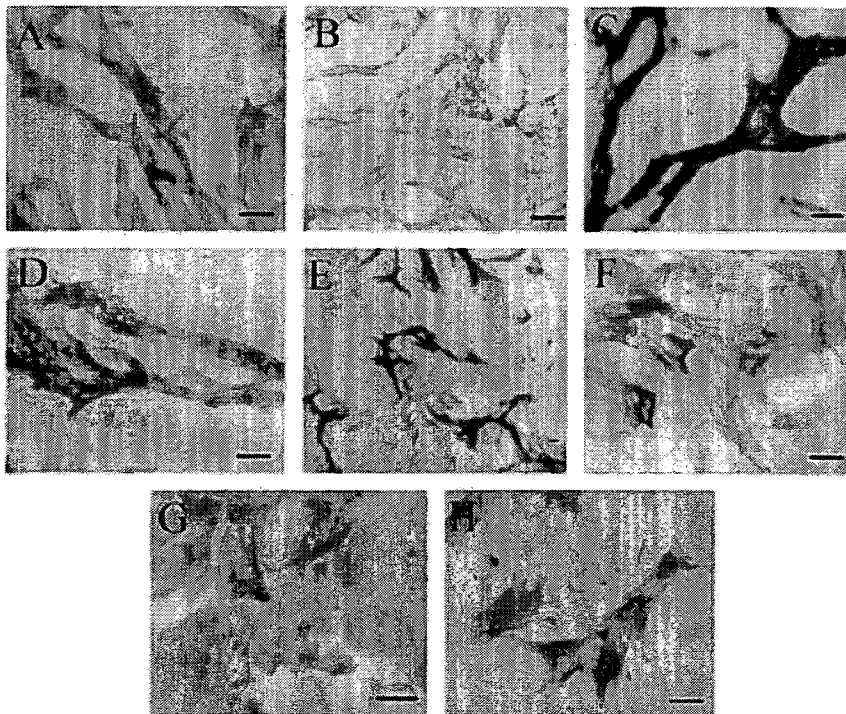


**Figure 2.** Immunocytochemical analysis of differentiation of vascular progenitor cells into vascular cells. A through D, Immunostaining for endothelial cell markers on VEGF-R2<sup>+</sup> TRA1-60<sup>-</sup> cells recultured with VEGF and FBS. A, CD34; B, VE-cadherin; C, CD31; D, endothelial NO synthase; E, Double immunostaining for CD31 (blue) and  $\alpha$ -smooth muscle actin (brown). F and G, Immunostaining for MC markers on VEGF-R2<sup>+</sup> TRA1-60<sup>-</sup> cells recultured with FBS. F,  $\alpha$ -Smooth muscle actin; G, Calponin; H, Immunostaining for  $\alpha$ -smooth muscle actin with treatment of PDGF-BB on VEGF-R2<sup>+</sup> TRA1-60<sup>-</sup> cells. Scale bars, 50  $\mu$ m.

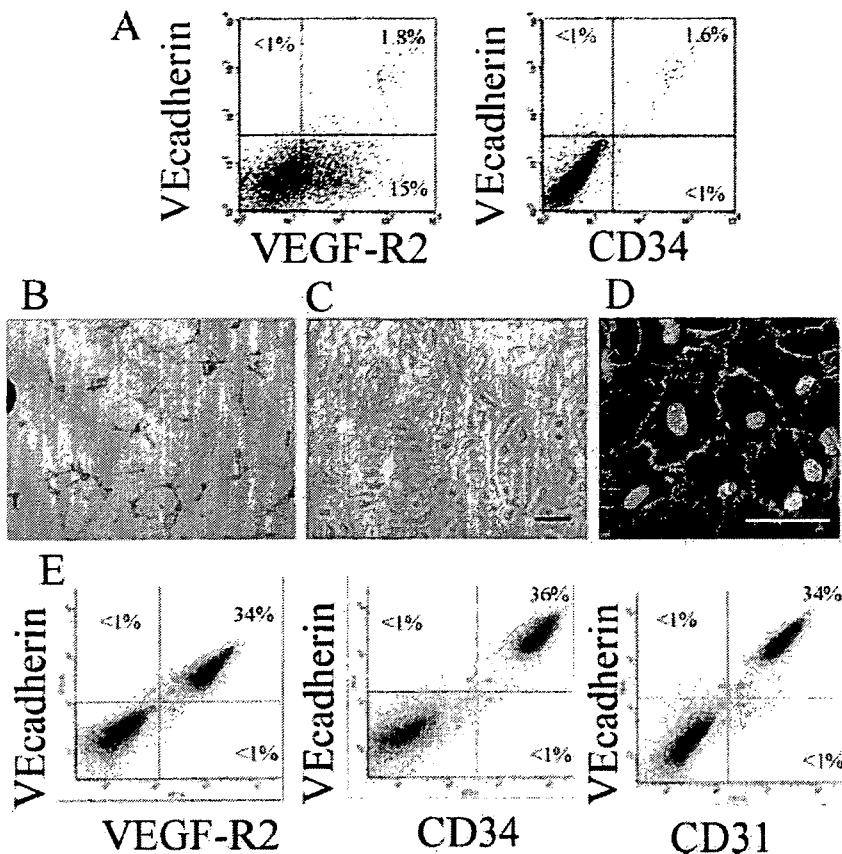


**Figure 3.** Isolation and expansion of vascular eECs. **A**, Flow-cytometric analysis of human ES cell-derived cells on an OP9 feeder layer on day 10. **B**, Network formation of human ES cell-derived VE-cadherin<sup>+</sup> cells (eECs) after 24-hour culture on Matrigel. **C**, Phase-contrast microscopic analysis of recultured VE-cadherin<sup>+</sup> cells on a collagen IV-coated dish. **D**, Immunostaining of recultured VE-cadherin<sup>+</sup> cells; red, CD31; green, nuclear staining (SYBR-Green I). **E**, Flow-cytometric analysis of the cells at the sixth passage expanded from VE-cadherin<sup>+</sup> cells. Scale bar, 50  $\mu$ m.

muscle actin expression (Figure 2E). In the absence of VEGF, VEGF-R2<sup>+</sup> TRA1-60<sup>-</sup> cells did not differentiate into ECs, but almost all of them differentiated into  $\alpha$ -smooth muscle actin and calponin-positive cells, which can be categorized as MCs (Figure 2F and 2G). Because these VEGF-R2<sup>+</sup> TRA1-60<sup>-</sup> cells expressed PDGFR $\beta$ , PDGF-BB with 0.5% FCS induced MC induction in a similar manner (Figure 2H). We, therefore, concluded that these VEGF-R2<sup>+</sup> TRA1-60<sup>-</sup> cells could be categorized as human VPCs that can differentiate into both ECs and MCs. Next we examined whether VEGF-R2<sup>+</sup> TRA1-60<sup>+</sup> cells after 8 days of differentiation is immature or not. Before differentiation, VEGF-R2<sup>+</sup> TRA1-60<sup>+</sup> cells were positive for flt1, AC133, and c-Kit and negative for CXCR4, PDGFR $\alpha$ , PDGFR $\beta$ , CD34, and VE-cadherin. However, after 8 days of differentiation, c-Kit expression decreased, and PDGFR $\alpha$ -positive and/or  $\beta$ -positive cells appeared in VEGF-R2<sup>+</sup> TRA1-60<sup>+</sup> cells (data not shown). Thus, VEGF-R2<sup>+</sup> TRA1-60<sup>+</sup> cells after 8 days of differentiation were not equivalent to the immature ES cells on day 0.

#### Isolation and Expansion of Vascular eECs

Next, we focused our attention on VE-cadherin<sup>+</sup> ECs that were more differentiated than the VPC. On 10 days of differentiation of HES3 on an OP9 feeder layer, VEGF-R2<sup>+</sup> and VE-cadherin<sup>+</sup> cells emerged and accounted for  $\approx$ 1% to 2% of all the cells (Figure 3A). This VE-cadherin-positive cell population was almost identical to the CD34<sup>+</sup> population (Figure 3A). We sorted these VE-cadherin<sup>+</sup> cells, and, be-

cause these cells were also VEGF-R2<sup>+</sup> and CD34<sup>+</sup> (Figure 3A), we used the term "eEC" for these EC in the early differentiation stage. These cells formed a network-like structure on Matrigel in vitro (Figure 3B), showed a cobblestone appearance when they became confluent (Figure 3C), and immunofluorescence staining with CD31 showed a characteristic marginal staining pattern (Figure 3D). These eECs were negative for monocyte makers CD45, CD11b, and CD14 (data not shown) and could be successfully propagated by a factor of  $\approx$ 1.2 $\times$ 10<sup>2</sup> (from 2 $\times$ 10<sup>5</sup> cells to 2.4 $\times$ 10<sup>7</sup> cells) after 6 passages on collagen IV-coated dishes. They were cultured with a cell density of 1.5 $\times$ 10<sup>4</sup> cells/cm<sup>2</sup> with VEGF because they did not expand when they were more sparsely plated or cultured without VEGF. Flow-cytometric analysis showed that VE-cadherin<sup>+</sup> cells were reduced to  $\approx$ 35% of the total number of cells after 6 passages (Figure 3E), but they were still VEGF-R2<sup>+</sup>, CD34<sup>+</sup>, and CD31<sup>+</sup> at the sixth passage, indicating that the cell differentiation stage had been maintained (Figure 3E). In another series of experiments, we sorted these VE-cadherin<sup>+</sup> cells on day 10 and replated them on an OP9 feeder layer or nonfeeder collagen IV-coated dishes for 1 additional week. The VE-cadherin<sup>+</sup> cells in these 2 culture groups were then resorted and plated on nonfeeder collagen IV-coated dishes for reculturing. After an additional 3 weeks of reculturing, VE-cadherin expression was examined. The cells that were cultured for 1 additional week on OP9 were 90% positive for VE-cadherin, but the cells kept on nonfeeder dishes were only 44% positive. This suggests that VE-cadherin<sup>+</sup> eECs still retain the potential to differentiate

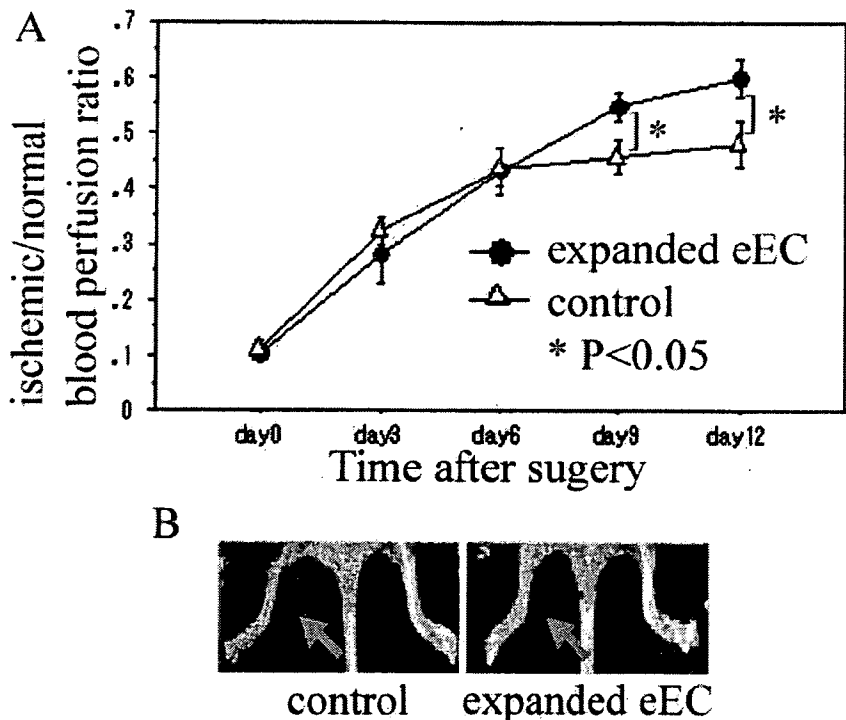


**Figure 4.** Transplantation of human ES cell-derived vascular cells to the hindlimb ischemia model of immunodeficient mice. **A**, Quantitative analysis of the hindlimb blood flow by means of calculating the ischemic/normal limb perfusion ratios in mice with ischemic hindlimb. \* $P < 0.05$ . On days 9 and 12, the blood flow in the ischemic limb of the expanded eEC-injected mice ( $n=8$ ) had increased significantly compared with that of control mice ( $n=8$ ). **B**, Representative laser Doppler perfusion images on day 12.

into other cell types, but more differentiated VE-cadherin<sup>+</sup> ECs may lose this ability.

#### Transplantation of Human ES Cell-Derived Vascular Cells to the Hindlimb Ischemia Model of Immunodeficient Mice

As the next step, we investigated whether human ES cell-derived vascular cells can be used for vascular regeneration in cell transplantation in the hindlimb ischemia model. KSN nude mice received an intra-arterial injection of cells in PBS or PBS only into the right femoral artery, followed by right femoral artery ligation and removal to create hindlimb ischemia. VEGF-R2<sup>+</sup> TRA1-60<sup>-</sup> cells, identified as VPCs, were transplanted, but laser Doppler perfusion image analysis on day 14 showed no significant difference in recovery of the blood flow (expressed as the ischemic/normal limb blood perfusion ratio) between the cell-transplanted mice ( $0.496 \pm 0.29$ ;  $n=10$ ) and the control PBS-injected mice ( $0.433 \pm 0.42$ ;  $n=14$ ). Next, we used the eECs expanded at passages 4 to 6. As shown in Figure 4A and 4B, the hindlimb blood flows had significantly improved in the cell-injected group 9 and 12 days after injection. For histological analysis, transplanted cells had been labeled with CM-DiI before cell transplantation, and biotin-conjugated isolectin B<sub>4</sub> was intravenously injected to stain ECs before sacrifice on day 14. Although some of the transplanted cells were incorporated as isolectin B<sub>4</sub><sup>+</sup> vascular ECs in the large vessels (Figure 5A), most of the transplanted cells were incorporated as small capillaries (Figure 5B). To quantify the capillary density, sections of the ischemic hindlimbs were stained with anti-mouse and human-specific CD31 antibodies (Figure 5C and 5D). Human CD31<sup>+</sup> capillaries were detected in the expanded eEC-transplanted mice. The

mouse and/or human CD31<sup>+</sup> total capillary number and area significantly increased in the expanded eEC-transplanted group compared with the control PBS-injected group, whereas there was tendency but no significant difference in the mouse CD31<sup>+</sup> host capillary number and area (Figure 5E and 5F). On the other hand, there was no significant difference in the capillary length (Figure 5G). Because we cut our sections at right angles with muscle fibers and femoral artery, it might be difficult to estimate the capillary density by vessel length.

Next we performed our transplantation experiments with the same procedure using BALB/c Slc nude mice, in which hindlimb ischemia is more severe than in KSN/Slc nude mice. PBS, VPCs, eECs or human adult aortic ECs were transplanted, and the ischemic hindlimbs were observed on day 14. In the PBS-injected mice, the ischemic hindlimb was autoamputated in 3 of 7 mice, and mild necrosis was observed in 1 of 7. In the VPC-transplanted mice, 3 of 7 were autoamputated and mild necrosis was seen in 2 of 7. In the eEC-transplanted mice, the ischemic hindlimb was not autoamputated, and only mild necrosis was observed in 2 of 8. In the human adult aortic EC-transplanted mice, 4 of 7 were auto-amputated, and mild necrosis was seen in 1 of 7. Furthermore, sections of the ischemic hindlimb in mice without autoamputation were stained with anti-mouse and human-specific CD31 antibodies. Human CD31<sup>+</sup> capillaries were most abundant in the eEC-transplanted mice, although some human CD31<sup>+</sup> cells were detected in the VPC or human adult aortic EC-transplanted mice (please see <http://atvb.ahajournals.org>).

#### Exclusion of Possible Teratoma Formation by the Expanded eEC

Further experiments were conducted to detect possible teratoma formation by eEC. We conducted long-term follow-ups

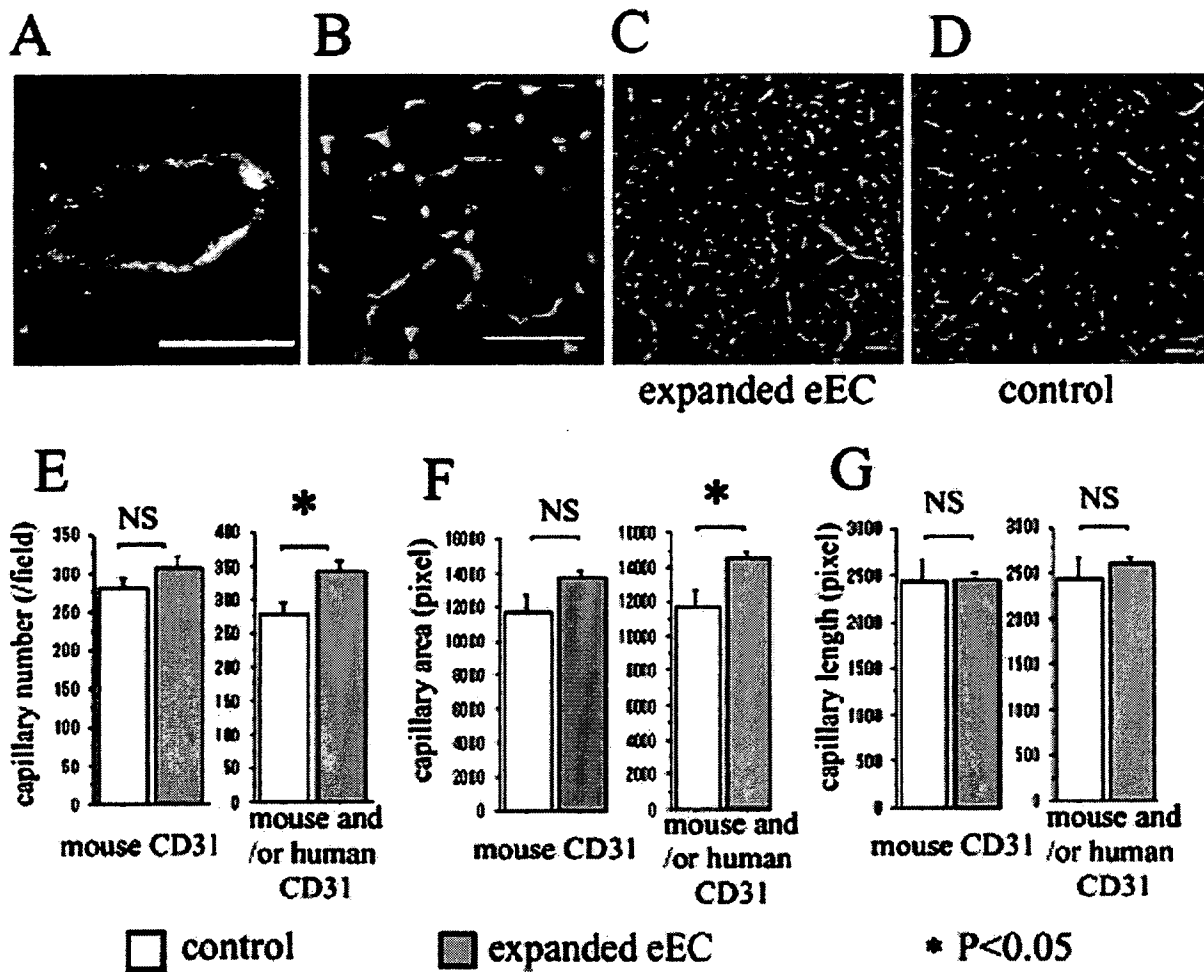


**Figure 5.** A and B, Histological analysis of vascular regeneration by the intra-arterially injected expanded eEC; green, isolectin B<sub>4</sub><sup>+</sup> endothelial cells; red, CM-Dil<sup>+</sup> transplanted cells (representative photographs). C and D, Fluorescent photographs of ischemic hindlimb for capillary density analysis; green, mouse CD31<sup>+</sup> capillaries; red, human CD31<sup>+</sup> capillaries (representative photographs). E through G, Quantitative analysis of the mouse and human endothelial cell marker-positive capillary densities in the ischemic hindlimb. E, capillary numbers. F, capillary areas. G, capillary lengths. Scale bars, 50  $\mu$ m.

by transplanting expanded eECs or undifferentiated human ES cells into 3 mice each and following them for 5 months. We transplanted  $5 \times 10^5$  cells under the dorsal back skin of SCID mice, which are commonly used for teratoma formation for human ES cells. Large tumors had formed after 3 to 5 months in 2 of the 3 mice in the human ES cell-transplanted group, but none had formed in any of the 3 mice in the expanded eEC-transplanted group. In immunohistological analysis, HLA-ABC<sup>+</sup> tumors were not observed in the subcutaneous region of eEC transplanted mice, although only a few HLA-ABC<sup>+</sup> human cells were remaining (data not shown).

**Expression of Angiogenic Factors in Human ES Cell-Derived Vascular Cells**

In addition, we investigated whether VPC or eEC produced major angiogenic factors such as VEGF, bFGF, human growth factor, and PDGF-BB. RT-PCR analysis detected mRNA expressions of VEGF, bFGF, and human growth factor in VPCs and PDGF-B and bFGF in eECs (please see <http://atvb.ahajournals.org>). We measured the protein con-

centration of these angiogenic factors in culture media by ELISA; however, the concentration of VEGF, human growth factor, and PDGF-BB did not reached the detectable level, and the concentration of bFGF was <30 pg/mL.

**Discussion**

In this study, we were able to clarify the differentiation process from human ES cells to mature vascular cell components. In adults, VEGF and PDGF receptors are expressed on EC and MC, respectively, and VEGF and PDGF stimulate the growth of the respective cell types. In this study, human ES cell-derived VPCs expressed both VEGF and PDGF receptors. In addition, stimulation with VEGF and PDGF-BB induced 2 differentiation pathways for EC and MC in this cell population. In mouse embryos, VEGF-R2 and PDGFR $\alpha$  were reported to be expressed in the mesoderm.<sup>11</sup> In whole-mount immunohistochemistry of mouse embryos (E7.5 to 8), VEGF-R2 was expressed predominantly in the extraembryonic and proximal-lateral mesoderm. PDGFR $\alpha$  was detected mainly in the paraxial embryonic mesoderm. Both VEGF-R2 and PDGFR $\alpha$  were

detected in the anterior paraxial mesoderm. It was also reported that vascular endothelial precursors were identified from the cephalic mesoderm of the avian embryo labeled using an antibody against Quek1 (avian homolog of VEGF-R2).<sup>12</sup> Our result that VEGF-R2<sup>+</sup> PDGFR<sup>+</sup> VPCs can differentiate into vascular cells may agree with their reports. In our transplantation examination, some human CD31<sup>+</sup> ECs were observed in the ischemic hindlimb of VPC-transplanted mice. This suggests that some transplanted VPC (negative for CD31) differentiated into CD31<sup>+</sup> ECs in vivo.

In addition, we investigated whether human ES cell-derived vascular cells can be used for vascular regeneration. Transplanted eECs were successfully incorporated into the host circulation and significantly accelerated improvement of local blood flow, whereas VPCs did not. We reported recently that VEGF-R2<sup>+</sup> cells derived from mouse ES cells could differentiate into not only vascular cells but also cardiomyocytes.<sup>13</sup> Thus, VPCs may be too immature to be used directly as the source for vascular regeneration. It has also been reported that ischemia-induced neovascularization did not improve in mice receiving human mature ECs (eg, human microvascular ECs).<sup>14</sup> Their report is compatible with our result that human adult aortic EC transplantation had no effect for the prevention of ischemic necrosis. The induction and isolation of the cells at the differentiation stage most appropriate for transplantation seem to be important. Judging from our results obtained from histological analysis and capillary density evaluation, at least some of the therapeutic effect of transplantation of expanded eECs could be attributed to vascular regeneration as a result of incorporation of the transplanted cells into the host vessels. Because RT-PCR analysis detected mRNA expression of PDGF-B not in VPCs but in eECs, PDGF-BB secretion might affect the effect of eEC transplantation, although PDGF-BB did not reach the detectable level in culture media. In adults, endothelial progenitor cells (EPCs) reportedly participate in postnatal angiogenesis,<sup>15</sup> whereas other reports suggest that EPCs contribute to neovascularization in tissue ischemia.<sup>14</sup> However, the expansion of EPCs in sufficient quantities to improve blood flow in large animals has not yet been achieved. In addition, some recent reports suggest that adult bone marrow-derived cells, such as EPCs, do not transdifferentiate into ECs under physiological conditions.<sup>16,17</sup> Although the role of EPCs as a modifier of vascular growth awaits further investigation, our findings may help provide an alternative and novel supply of vascular cells for cell therapy as a contribution to vascular regenerative medicine.

Furthermore, the establishment of an in vitro differentiation system of human vascular cell components from human ES cells in this study should also make it possible to dissect out cellular mechanisms in human vascular development and diseased states for which the knockout animal research approach is not practical. Trials on gene expression profiling using our in vitro differentiation system of human vascular cells from human ES cells could assist in the search for novel

gene products to develop new therapeutic approaches for vascular regeneration.

### Acknowledgments

The human ES cells (HES-3) were contributed by ES Cell International Pte Ltd, Singapore. The anti-human VEGF-R2 antibody (KM1668) was a generous gift from M. Shibuya, MD, PhD, Department of Cancer Biology, Institute of Medical Science, University of Tokyo.

### Sources of Funding

This work was supported by Grants-in-Aid for Scientific Research from the Ministry of Health, Labour and Welfare and the Ministry of Education, Culture, Sports, Science and Technology. This work was also supported by a grant from the Japan Smoking Foundation, a Japan Heart Foundation/Pfizer Japan Grant for Cardiovascular Disease Research, and a grant from the Study Group for Molecular Cardiology Research. This work was also supported by Fellowships of the Japan Society for the Promotion of Young Scientists and Establishment of International COE for Integration of Transplantation Therapy and Regenerative Medicine (COE program of the Ministry of Education, Culture, Sports, Science and Technology, Japan).

### Disclosures

None.

### References

1. Reubinoff BE, Pera MF, Fong CY, Trounson A, Bongso A. Embryonic stem cell lines from human blastocysts: somatic differentiation in vitro. *Nature Biotechnology*. 2000;18:399–404.
2. Yamashita J, Itoh H, Hirashima M, Ogawa M, Nishikawa S, Yurugi T, Naito M, Nakao K, Nishikawa S. Flk1-positive cells derived from embryonic stem cells serve as vascular progenitors. *Nature*. 2000;408:92–96.
3. Miyashita K, Itoh H, Sawada N, Fukunaga Y, Sone M, Yamahara K, Yurugi-Kobayashi T, Park K, Nakao K. Adrenomedullin provokes endothelial Akt activation and promotes vascular regeneration both in vitro and in vivo. *FEBS Lett*. 2003;544:86–92.
4. Yurugi-Kobayashi T, Itoh H, Schroeder T, Nakano A, Narazaki G, Kita F, Yanagi K, Hiraoka-Kanie M, Inoue E, Ara T, Nagasawa T, Just U, Nakao K, Nishikawa S, Yamashita J, Nishikawa S. Adrenomedullin/cyclic amp pathway induces notch activation and differentiation of arterial endothelial cells from vascular progenitors. *Arterioscler Thromb Vasc Biol*. 2006;26:1977–1984.
5. Kaufman DS, Hanson ET, Lewis RL, Auerbach R, and Thomson JA. Hematopoietic colony-forming cells derived from human embryonic stem cells. *Proc Natl Acad Sci U S A*. 2001;98:10716–10721.
6. Levenberg S, Golub JS, Amit M, Itskovitz-Eldor J, Langer R. Endothelial cells derived from human embryonic stem cells. *Proc Natl Acad Sci U S A*. 2002;99:4391–4396.
7. Fujioka T, Yasuchika K, Nakamura Y, Nakatsuji N, Suemori H. A simple and efficient cryopreservation method for primate embryonic stem cells. *Int J Dev Biol*. 2004;48:1149–1154.
8. Hirashima M, Kataoka H, Nishikawa S, Matsuyoshi N, Nishikawa S. Maturation of embryonic stem cells into endothelial cells in an in vitro model of vasculogenesis. *Blood*. 1999;93:1253–1263.
9. Yamahara K, Itoh H, Chun TH, Ogawa Y, Yamashita J, Sawada N, Fukunaga Y, Sone M, Yurugi-Kobayashi T, Miyashita K, Tsujimoto H, Kook H, Feil R, Garbers DL, Hofmann F, Nakao K. Significance and therapeutic potential of the natriuretic peptides/cGMP/cGMP-dependent protein kinase pathway in vascular regeneration. *Proc Natl Acad Sci U S A*. 2003;100:3404–3409.
10. Sone M, Itoh H, Yamashita J, Yurugi-Kobayashi T, Suzuki Y, Kondo Y, Nonoguchi A, Sawada N, Yamahara K, Miyashita K, Park K, Shibuya M, Nito S, Nishikawa S, Nakao K. Different differentiation kinetics of vascular progenitor cells in primate and mouse embryonic stem cells. *Circulation*. 2003;107:2085–2088.
11. Kataoka H, Takakura N, Nishikawa S, Tsuchida K, Kodama H, Kunisada T, Risau W, Kita T, Nishikawa S. Expressions of PDGF receptor alpha, c-Kit and Flk1 genes clustering in mouse chromosome 5 define distinct

- subsets of nascent mesodermal cells. *Dev Growth Differ.* 1997;39:729–740.
12. Couly G, Coltey P, Eichmann A, Le Douarin NM. The angiogenic potentials of the cephalic mesoderm and the origin of brain and head blood vessels. *Mech Dev.* 1995;53:97–112.
  13. Yamashita JK, Takano M, Hiraoka-Kanie M, Shimazu C, Peishi Y, Yanagi K, Nakano A, Inoue E, Kita F, Nishikawa S. Prospective identification of cardiac progenitors by a novel single cell-based cardiomyocyte induction. *FASEB J.* 2005;19:1534–1536.
  14. Kalka C, Masuda H, Takahashi T, Kalka-Moll WM, Silver M, Kearney M, Li T, Isner JM, Asahara T. Transplantation of ex vivo expanded endothelial progenitor cells for therapeutic neovascularization. *Proc Natl Acad Sci U S A.* 2000;97:3422–3427.
  15. Asahara T, Murohara T, Sullivan A, Silver M, van der Zee R, Li T, Witzenbichler B, Schatteman G, Isner JM. Isolation of putative progenitor endothelial cells for angiogenesis. *Science.* 1997;275:964–967.
  16. O'Neill TJ 4th, Wamhoff BR, Owens GK, Skalak TC. Mobilization of bone marrow-derived cells enhances the angiogenic response to hypoxia without transdifferentiation into endothelial cells. *Circ Res.* 2005;97:1027–1035.
  17. Zentilin L, Tafuro S, Zacchigna S, Arsic N, Pattarini L, Sinigaglia M, Giacca M. Bone marrow mononuclear cells are recruited to the sites of VEGF-induced neovascularization but are not incorporated into the newly formed vessels. *Blood.* 2006;107:3546–3554.

# Therapeutic Potential of Atrial Natriuretic Peptide Administration on Peripheral Arterial Diseases

Kwijun Park, Hiroshi Itoh, Kenichi Yamahara, Masakatsu Sone, Kazutoshi Miyashita, Naofumi Oyamada, Naoya Sawada, Daisuke Taura, Megumi Inuzuka, Takuhiro Sonoyama, Hirokazu Tsujimoto, Yasutomo Fukunaga, Naohisa Tamura, and Kazuwa Nakao

Department of Medicine and Clinical Science, Kyoto University Graduate School of Medicine, Kyoto 606-8507, Japan

Peripheral arterial diseases are caused by arterial sclerosis and impaired collateral vessel formation, which are exacerbated by diabetes, often leading to leg amputation. We have reported that an activation of the natriuretic peptides/cGMP/cGMP-dependent protein kinase pathway accelerated vascular regeneration and blood flow recovery in murine legs, for which ischemia had been induced by a femoral arterial ligation as a model for peripheral arterial diseases. In this study, ip injection of carperitide, a human recombinant atrial natriuretic peptide, accelerated blood flow recovery with increasing capillary density in ischemic legs not only in nondiabetic mice but also in mice kept upon streptozotocin-induced hyperglycemia for 16 wk, which significantly impaired the blood flow recovery compared with nondiabetic mice. Based on these findings, we tried to apply the administration of

carperitide to the treatment of peripheral arterial diseases. The study group comprised a continuous series of 13 patients with peripheral arterial diseases (Fontaine's classification I, one; II, five; III, two; and IV, five), for whom conventional therapies had not accomplished appreciable results. Carperitide was administered continuously and intravenously for 2 wk to Fontaine's class I–III patients and for 4 weeks to class IV patients. The dose was gradually increased to the maximum, with the patient's systolic blood pressure being kept above 100 mm Hg. Carperitide administration improved the ankle-brachial pressure index, intermittent claudication, rest pain, and ulcers. In conclusion, this study showed a therapeutic potential of carperitide to treat peripheral arterial diseases refractory to conventional therapies. (*Endocrinology* 149: 483–491, 2008)

**L**OWER EXTREMITY PERIPHERAL artery disease (PAD), which consists of arteriosclerosis thrombotica and thromboangiitis obliterans, is caused by the altered structure and function of the arteries that supply the lower limbs. Numerous pathophysiological processes can contribute to the creation of stenoses or aneurysms of peripheral artery circulation. Among them, diabetes mellitus is one of the most important causes of PAD. According to the Centers for Disease Control and Prevention's National Center for Chronic Disease Prevention and Health Promotion, 82,000 people have diabetes-related leg, foot, or toe amputations each year in the United States. World Diabetes Day announced that up to 70% of leg amputation cases are patients with diabetes. In PAD patients with diabetes, collateral vessel formation is impaired (1), and intricately modified angiogenesis contributes to a large variety of complications including diabetic gangrene (2). Mechanisms that alter angiogenesis in diabetes are largely unknown. It is reported, however, that either inappropriate production or action of nitric oxide (NO) may

play important roles in vascular insufficiencies with diabetes (3). NO activates soluble guanylyl cyclase (GC) followed by the cGMP signal transduction cascade (4). Significant reverse correlation between the urinary cGMP excretion rate and the disease grade according to Fontaine's classification observed in PAD patients seems to imply the impact of diminished cGMP production in PAD (5).

Natriuretic peptides (NPs) consist of atrial NP (ANP), brain NP (BNP), and C-type NP (CNP) and elicit various biological effects by activating particulate GCs: GC-A is a receptor selective for ANP and BNP, and GC-B is a receptor selective for CNP (4, 6–8). One of the major mediators of cGMP signaling is cGMP-dependent protein kinase (cGK) (4). ANP and BNP are secreted mainly from the atrium and ventricle of the heart, respectively, and act as cardiac hormones (4, 6, 7). The clinical significance of NPs is already recognized in the diagnosis and treatment of congestive heart failure (CHF). Recombinant human ANP and BNP are used for treating CHF, with the main expectation of diuretic and natriuretic effects (9, 10).

Recently, NPs have been revealed to have various effects on cell survival, proliferation, and differentiation. We reported that ANP at a physiological concentration induces endothelial regeneration in the human coronary artery and umbilical vein through the activation of ERK and phosphatidylinositol 3-kinase/Akt pathways (11). We used genetically engineered mice that overexpress BNP and type I cGK (cGKI), or otherwise lack cGKI, and demonstrated that BNP can promote vascular regeneration and accelerate the restoration of blood flow after the removal of a hind-limb artery in mice through the activation of the GC-A/cGMP/cGKI

First Published Online November 8, 2007

Abbreviations: ABI, Ankle-brachial pressure index; ADMA, asymmetric dimethylarginine; ANP, atrial natriuretic peptide; BNP, brain natriuretic peptide; cGK, cGMP-dependent protein kinase; cGKI, type I cGMP-dependent protein kinase; CHF, congestive heart failure; CNP, C-type natriuretic peptide; EC, endothelial cell; ESRD, end-stage renal disease; GC, guanylyl cyclase; NP, natriuretic peptide; PECAM, platelet endothelial cell adhesion molecule-1; SMC, smooth muscle cell; STZ, streptozotocin; VEGF, vascular endothelial growth factor.

*Endocrinology* is published monthly by The Endocrine Society (<http://www.endo-society.org>), the foremost professional society serving the endocrine community.



pathway (12–14). Meanwhile, CNP, which is secreted from endothelial cells (ECs) and acts as an endothelium-derived relaxing peptide (15), also induces redifferentiation of vascular smooth muscle cells (SMCs) while accelerating reendothelialization and suppressing neointimal hyperplasia in vein grafting or balloon injuries in rabbits, which simulate atherosclerotic lesions in humans (16, 17). These observations indicate that GC-A/cGMP and GC-B/cGMP signaling cascades have potential to promote vascular regeneration in PAD and to inhibit the progression of atherosclerotic lesions. On the other hand, we have reported previously that endothelial CNP expression is progressively reduced in accordance with the severity of human coronary atherosclerosis (18), which indicates that not only NO/soluble GC/cGMP signaling but also CNP/GC-B/cGMP signaling might be impaired in PAD. Therefore, the restoration of intracellular cGMP levels by the activation of GC-A, the third signaling pathway using cGMP as the second messenger in vascular SMCs and ECs, could improve PAD.

In this context, we hypothesized that an administration of ANP or BNP could, at least partly, compensate for impaired angiogenesis due to diminished intracellular cGMP levels in PAD patients by an activation of GC-A. In Japan, carperitide, a recombinant human ANP, is already approved and widely used for the treatment of CHF. By contrast, nesiritide, a recombinant human BNP, has not been approved in Japan, and it cannot be applied to rodent models because amino acid sequences and molecular forms of BNP are quite different between humans and rodents. In the present study, we therefore examined the effect of carperitide on vascular regeneration in animal models with diabetes, and we further tried to determine safety and to investigate any possible therapeutic effects of carperitide in PAD patients.

## Materials and Methods

### Animals

C57BL/6 male mice (CLEA Japan, Inc., Tokyo, Japan) were used for experiments. Diabetes was induced in the mice by repetitive (once a day for 4–6 consecutive days) ip injections of streptozotocin (STZ) (Nacalai Tesque Inc, Kyoto, Japan; 65–100 mg/kg body weight in 200  $\mu$ l of 10 mM sodium citrate buffer, pH 4.0) at 8 wk of age. Blood glucose concentrations were monitored weekly after STZ treatment with Dexter-ZII (Bayer Medical Ltd., Tokyo, Japan). Animals with blood glucose levels above 220 mg/dl at 2 wk after the first STZ injection were used as STZ-diabetic mice. Control mice received an equal volume of citrate buffer. Mice were used for experiments of limb ischemia at 4, 16, and 26 wk after the first injection of STZ or vehicle.

An animal model of limb ischemia was made by a ligation of one femoral artery. The blood flow in both legs was assessed with a laser Doppler perfusion image analyzer (Moor Instruments, Devon, UK), and the blood flow recovery was assessed by the ischemic limb to normal limb ratio of blood flow, as we described previously (14).

To assess the effect of carperitide, a recombinant human ANP (Daiichi Asubio Pharma Co., Ltd., Tokyo, Japan), on angiogenesis in ischemic limbs, the femoral artery ligation was carried out at 16 wk after the first injection of STZ or vehicle, and carperitide at a dose of 2.2  $\mu$ g/kg-min or equal volume of water (vehicle) was administered continuously and ip via a microosmotic pump (Alzet model 1002D; Alzet Pharmaceuticals, Palo Alto, CA), which was implanted ip at 3 d after the femoral artery ligation. Pumps were renewed at d 14 after primary implantation. At 28 d from the femoral artery ligation, mice were euthanized by an overdose of pentobarbital injection, and the ischemic hind limb was isolated for the histological analysis.

All experimental procedures were performed according to Kyoto University standards for animal care.

### Histological analysis

After fixation with 4% paraformaldehyde, ischemic lower legs were embedded in OCT compound (Sakura Finetechnical, Tokyo, Japan) and frozen at  $-80^{\circ}\text{C}$ . Cryostat sections (4–8  $\mu$ m thick) of the tissue were stained with a rat antimouse platelet EC adhesion molecule-1 (PECAM-1) antibody (item 553370; PharMingen, San Diego, CA). Four random fields on two different sections (3 mm apart) from each mouse were photographed with a digital camera (Olympus, Tokyo, Japan). By computer-assisted analysis using NIH IMAGE, capillary density was calculated as the mean number of capillaries stained with PECAM-1, as we described previously (14).

### Patients

Participants were a series of 13 Japanese patients including 11 males and two females, aged 38–92 yr, who had already been diagnosed with PAD and hospitalized in our department from June 2003 to August 2005 (Table 1). Patients classified as Fontaine's classes II–IV or with characteristic symptoms of PAD were included. Diseases accompanying PAD were defined as follows: type 2 diabetes mellitus, following the diagnostic criteria of Japan Diabetes Society; hypertension, blood pressure is equal to or greater than 140/90 mm Hg; end-stage renal disease, chronic renal failure on indispensable renal replacement therapy; ischemic heart disease, history of angina pectoris or myocardial ischemia with or without present medication; CHF, past diagnosis of CHF with or without present medication; hyperlipidemia, low-density lipoprotein-cholesterol is equal to or greater than 140 mg/dl, or triglyceride is equal to or greater than 150 mg/dl; obesity, body mass index is greater than 25  $\text{kg}/\text{m}^2$ . Exclusion criteria were contraindications for carperitide: possibility of immediate surgery, suffering from malignancy, febrility, an inability to declare subjective symptoms, pregnancy, or other unfavorable statuses. The study was conducted in accordance with the guidelines in the Declaration of Helsinki. The study protocol was approved by the Ethics Committee Graduate School and Faculty of Medicine, Kyoto University. Patients were fully informed of the aim of the study, and their written informed consent was obtained.

### Procedure of carperitide administration to patients

Carperitide was administered continuously and iv for 2 wk for Fontaine I–III patients and for 4 wk for Fontaine IV patients in principle. The starting dose of 0.006  $\mu$ g/kg-min was gradually increased as long as the systolic blood pressure remained above 100 mm Hg. The range of final

TABLE 1. Patients' characteristics

Characteristic	n
Sex	
Male	11
Female	2
Diagnosis	
Arteriosclerosis obliterans	12
Thromboangitis obliterans	1
Gangrene or ulcer(s)	4
Fontaine's classification	
I	1
II	5
III	2
IV	5
Other disorders	
Hypertension	12
Type 2 diabetes	11
ESRD	7
CHF	5
Ischemic heart disease	4
Hyperlipidemia	4
Obesity (BMI > 25)	3

Patients' mean  $\pm$  SD age was 72  $\pm$  15 yr. BMI, Body mass index.

doses of carperitide used in this study was 0.003–0.1  $\mu\text{g}/\text{kg}\cdot\text{min}$ . Drugs for injection such as prostaglandins were avoided during the carperitide administration. The administration was stopped and standard remedy performed if any unfavorable symptoms appeared.

Pain was assessed when present with a numerical rating scale from 0–10; grade 0 indicated no pain and grade 10 the strongest pain the patient could imagine. The ankle-brachial pressure index (ABI) was assessed by an automated measurement device (BP-203RPEII; Colin Medical Technology Corp., Aichi, Japan). An exercise tolerance test was carried out weekly for patients with intermittent claudication. Pain-free walking distance on a flat ground was assessed. A stair-climb test was performed when walking on flat ground did not induce claudication. The test assessed how many floors a patient could climb without pain on the stair of our internal medicine ward building. Blood sampling was performed immediately before the beginning of carperitide administration and weekly during the administration for routine blood examination. It was also performed to determine the plasma levels of ANP, cGMP, and vascular endothelial growth factor (VEGF).

### Analysis of blood samples

The blood samples from mice were withdrawn in an ice-cold tube containing 0.5 M Na<sub>2</sub>EDTA final concentration and mixed well. Aprotinin was added at 500 U/ml when a sample was used for human ANP measurement. The plasma was immediately isolated by a centrifugation and stored at  $-20\text{ }^{\circ}\text{C}$  until further processing. Plasma concentrations of cGMP, VEGF, and human ANP were analyzed by SRL, Inc. (Tokyo, Japan).

### Statistical analysis

Results are presented as mean  $\pm$  SEM unless otherwise indicated. The statistical significance of differences in means was evaluated by ANOVA supplemented with Fisher's least-significant difference in comparisons among three or more groups in animal experiments and by paired *t* tests between before and after the carperitide administration in the human study. A *P* value  $< 0.05$  was considered significant.

## Results

### Animal experiments

#### Angiogenesis was impaired in diabetic mice

Blood glucose levels in STZ-diabetic mice, on which the hind-limb ischemia was induced at 4, 16, and 26 wk after STZ injections, were  $354 \pm 151$  mg/dl ( $n = 9$ ),  $354 \pm 38$  mg/dl ( $n = 9$ ), and  $308 \pm 23$  mg/dl ( $n = 9$ ), respectively, on the day of surgery. In control nondiabetic mice, blood glucose levels at 4 wk after the injection of vehicle were  $139 \pm 4$  mg/dl ( $n = 6$ ),  $132 \pm 2$  mg/dl ( $n = 9$ ), and  $131 \pm 4$  mg/dl ( $n = 9$ ) for mice operated at 4, 16, and 26 wk, respectively, after the vehicle injection.

At 4 wk after the induction of diabetes, blood flow recovery of the STZ-diabetic group was similar to that of nondiabetic controls (Fig. 1A). But after a long-term hyperglycemic state of 16 or 26 wk, recovery was suppressed in the STZ-diabetic group by 26 or 32%, respectively, when compared with the control mice (Fig. 1, B and C).

#### ANP administration restored angiogenesis in diabetic mice

To investigate whether ANP can improve the impairment of blood flow recovery, carperitide was administered to C57BL/6 mice in which femoral artery ligation was made after a 16-wk exposure to hyperglycemia.

Blood glucose levels at femoral artery ligation were  $116 \pm 4$  mg/dl in the vehicle-treated nondiabetic group,  $122 \pm 3$  mg/dl in the carperitide-treated nondiabetic group,  $343 \pm 42$

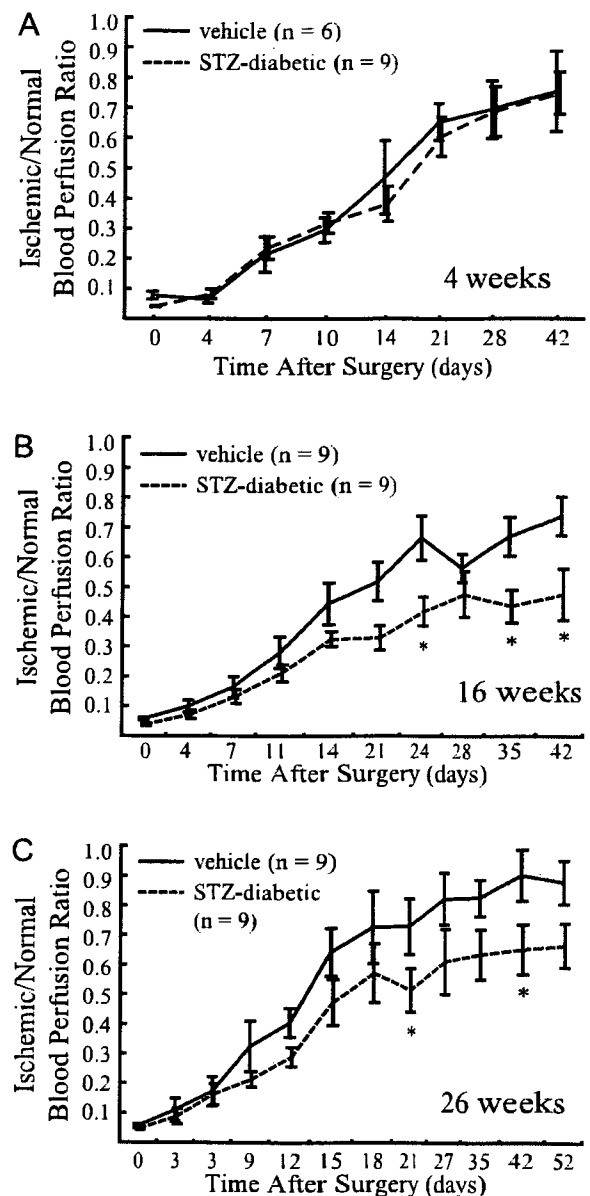


FIG. 1. Impairment of ischemia-induced blood flow recovery in mice with diabetes. Blood flow recovery after femoral artery ligation assessed by an ischemic/normal blood perfusion ratio was not altered 4 wk after STZ administration (A) but was significantly delayed 16 wk (B) and 26 wk (C) after induction of diabetes compared with vehicle-treated nondiabetic controls. \*,  $P < 0.05$  vs. vehicle-treated mice at each time point by ANOVA.

mg/dl in the vehicle-treated STZ-diabetic group, and  $366 \pm 42$  mg/dl in the carperitide-treated STZ-diabetic group. In nondiabetic mice, the carperitide administration significantly accelerated blood flow recovery compared with the vehicle-treated group. The ischemic/normal limb blood flow ratio measured at 21 d after the surgery was  $0.58 \pm 0.03$  in the vehicle-treated nondiabetic group ( $n = 13$ ) and was significantly augmented in the carperitide-treated nondiabetic group ( $0.74 \pm 0.06$ ,  $n = 7$ ;  $P < 0.05$ ). The accelerating effect of carperitide on blood flow recovery was also seen in STZ-diabetic mice. The ischemic/normal limb blood flow ratio at

21 days after surgery was  $0.52 \pm 0.05$  in the carperitide-treated STZ-diabetic group ( $n = 8$ ) and significantly higher than that in the vehicle-treated STZ-diabetic group ( $0.37 \pm 0.06$ ,  $n = 7$ ;  $P < 0.05$ ) (Fig. 2B). The time course of blood flow recovery in each group was shown in Fig. 2A.

In the vehicle-treated STZ-diabetic group, the capillary density was  $907 \pm 69$  counts/mm<sup>2</sup> ( $n = 6$ ) and was more significantly reduced than in the vehicle-treated nondiabetic group ( $1406 \pm 98$  counts/mm<sup>2</sup>,  $n = 6$ ;  $P < 0.05$ ) (Fig. 2, C and D). The capillary density tended to be higher in the carperitide-treated nondiabetic group ( $1604 \pm 108$  counts/mm<sup>2</sup>,  $n = 6$ ) than in the vehicle-treated nondiabetic group. Among STZ-diabetic mice, the carperitide administration significantly increased the capillary density to  $1180 \pm 95$  counts/mm<sup>2</sup> ( $n = 6$ ;  $P < 0.05$ ).

In this study, 4-wk administration of carperitide to mice increased plasma human ANP levels from under the detection limit (10 pg/ml) to  $156 \pm 79$  pg/ml ( $n = 5$  each) and plasma cGMP levels from  $8.9 \pm 1.1$  nM ( $n = 7$ ) to  $20.0 \pm 2.9$  nM ( $n = 6$ ,  $P < 0.05$ ). The carperitide administration altered blood pressure from  $106 \pm 3/73 \pm 3$  mm Hg to  $94 \pm 4/62 \pm 4$  mm Hg ( $n = 4$  each;  $P < 0.05$ ).

### Human study

All patients had characteristic symptoms of PAD (Fontaine's class: I, one; II, five; III, two; and IV, five) (Table 2). A patient who was Fontaine's class I had a cold sensation in the lower extremities. The diagnosis was confirmed by ABI measurement, ultrasound velocity spectroscopy, or magnetic resonance angiography.

Hypertension and diabetes were the two most frequent underlying diseases among participants (Table 1). Among diabetic subjects, HbA1c levels were  $7.7 \pm 0.5\%$ , and disease duration was  $16.5 \pm 2.1$  yr. Seven patients suffered from end-stage renal diseases and were on hemodialysis. Eight patients had a past history of an ischemic heart disease, CHF, or both, and all of them were in stable condition with or without medication. Plasma ANP levels were  $315 \pm 130$  pg/ml, and ejection fractions measured by ultrasonic echocardiography were  $49.9 \pm 6.2\%$ .

Plasma ANP levels were elevated from  $224 \pm 93$  pg/ml at baseline to  $400 \pm 125$  pg/ml during the administration ( $n = 12$ ;  $P < 0.05$ ; data were lacking in patient 5). Plasma cGMP levels were elevated from  $14.4 \pm 3.5$  to  $24.0 \pm 4.5$  nM ( $n =$

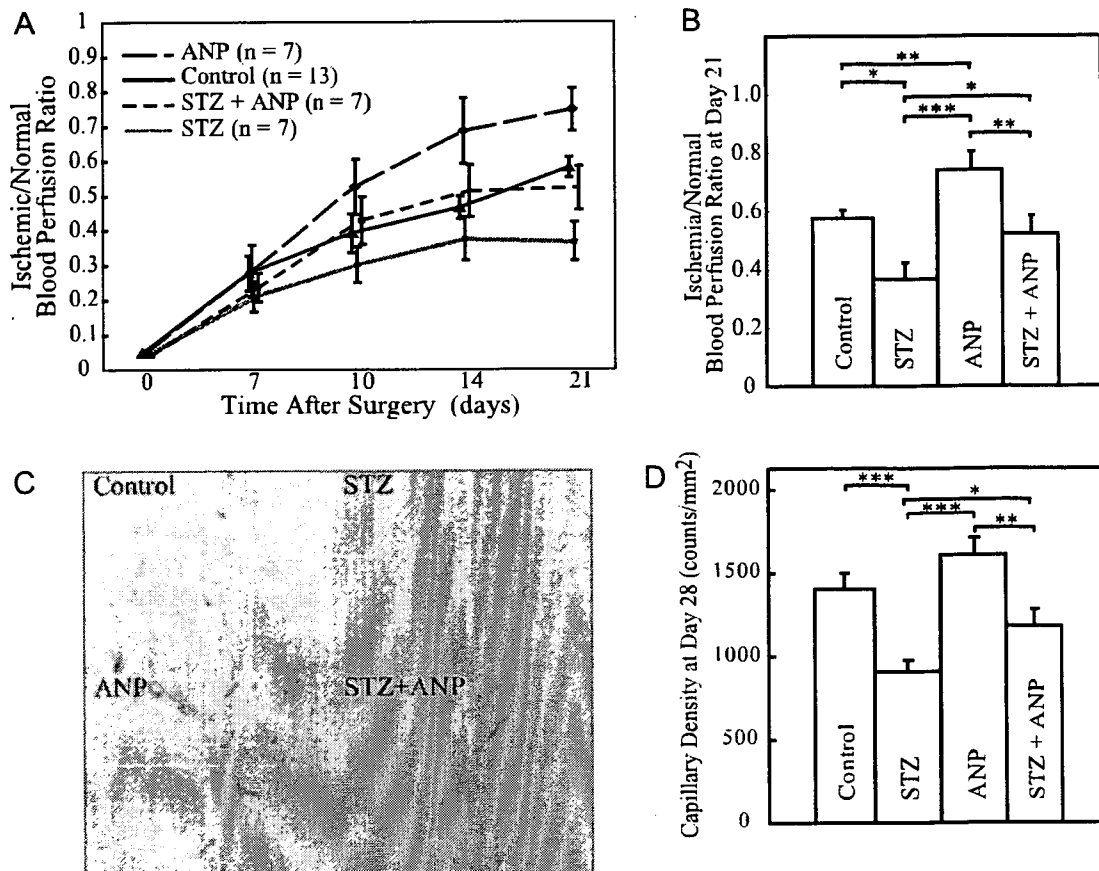


FIG. 2. Acceleration of ischemia-induced vascular regeneration by continuous ip administration of carperitide in nondiabetic and diabetic mice. A, Time course of ischemic/normal blood perfusion ratios measured by laser Doppler imaging; B, Calculated ischemic/normal blood perfusion ratios on d 21; C, immunostaining of the ischemic hind-limb tissue with anti-PECAM-1 antibody (bright red) at 28 d after the induction of ischemia; D, quantitative analysis of capillary density assessed by the immunostaining of PECAM-1. Control, Vehicle-treated nondiabetic; STZ, vehicle-treated STZ-diabetic; ANP, carperitide-treated nondiabetic; STZ + ANP, carperitide-treated STZ-diabetic. \*,  $P < 0.05$ ; \*\*,  $P < 0.01$ ; \*\*\*,  $P < 0.001$ .

**TABLE 2.** Detailed patients' characteristics

Patient no.	Diagnosis	Age (yr)/sex	Fontaine's class	Accompanying disease	Symptoms	RP rating	Exercise tolerance	Plasma ANP levels (pg/ml)	Medication
1	ASO	69/M	III	ESRD, DM, HT, IHD	RP	3	NA	79	Ap, P, C
2	TAO	38/F	II	DM, Ob	IC	NA	290	<5	Ap, P, V
3	ASO	82/F	I	DM, HT, Ob, HL, CHF	CS	NA	NA	16	An, Ap, P, V
4	ASO	77/M	IV	ESRD, HT, CHF	UI/RP	5	NA	668	An, Ap, P
5	ASO	90/M	IV	DM, HT	UI/RP	4	NA	152	P, V
6	ASO	85/M	IV	ESRD, DM, HT	UI/RP	NA	NA	51	An, C, N, V
7	ASO	76/M	II	DM, HT, Ob, HL	IC	NA	240	22	An, Ap, V
8	ASO	75/M	II	DM, HT, HL, IHD	IC	4	200	36	An, Ap, P, V
9	ASO	63/M	III	ESRD, HT	RP	NA	NA	97	An, Ap, P, V
10	ASO	92/M	II	ESRD, DM, HT, CHF	IC	NA	100	922	Ap, N, P
11	ASO	71/M	IV	ESRD, DM, HT, CHF	UI	NA	NA	645	Ap
12	ASO	57/M	II	DM, HT, HL, IHD	IC	3	5F	14	Ap, C, V
13	ASO	55/M	IV	ESRD, DM, HT, CHF, IHD	UI/RP		NA	137	An, Ap, P, V

For patient 12, exercise tolerance was assessed by a stair-climb test, the floor number of stair-climbing without pain was 5. Medications were continued during carperitide injection without a change. An, Angiotensin-converting enzyme inhibitor or angiotensin receptor blocker; Ap, antiplatelet; ASO, arteriosclerosis obliterans; C, cilostazol; CS, cold sensation of the peripheral; DM, type 2 diabetes mellitus; F, female; 5F, five floors; HL, hyperlipidemia; HT, hypertension; IC, intermittent claudication; IHD, ischemic heart disease; M, male; N, nitrate; NA, not applicable; Ob, obesity; P, prostanoid; RP, rest pain; TAO, thromboangitis obliterans; UI, gangrene or non-healing ulcer(s); V, vasodilator.

9;  $P < 0.01$ ). No significant differences were seen in plasma VEGF levels:  $92.2 \pm 25.4$  pg/ml at the baseline and  $65.2 \pm 11.1$  pg/ml in the course of administration ( $n = 8$ ). The blood pressure of patients (excepting those on hemodialysis) fell from  $143 \pm 8/74 \pm 2$  mm Hg to  $123 \pm 7/69 \pm 3$  mm Hg ( $n = 5$ ;  $P < 0.05$ ). An excessive decrease in systolic blood pressure to less than 90 mm Hg was observed in a few patients on hemodialysis and could be quickly reversed by reducing the carperitide infusion rate. Medications except for injections were continued during carperitide injection without any changes. Details of medications especially for PAD are shown in Table 2. Alprostadil (prostaglandin E) had been iv administered daily for a week to patients 2 and 3, and for a month to patients 6 and 11, and was stopped at least 3 d before the beginning of carperitide administration. Phosphodiesterase inhibitors other than cilostazol were not used in patients enrolled in this study. Smoking status was not changed in five never-smokers (patients 1, 3, 5, 12, and 13) and seven former smokers (patients 2, 4, 7, 8, 9, 10, and 11) during this study. One patient (no. 6) was a current smoker (20 cigarettes/d) at the enrollment and stopped smoking 7 d before the administration.

The ABI of the affected limb (or worse side when both limbs affected) was significantly elevated from  $0.61 \pm 0.08$  at the baseline to  $0.72 \pm 0.09$  on the 14th day of administration ( $n = 12$ ;  $P < 0.05$ ) except for patient 5, for whom the administration was stopped within a week (Table 3 and Fig. 3b). Brachial systolic blood pressure values for ABI calculations before and on the 14th day of administration were  $140 \pm 10$  and  $132 \pm 8$  mm Hg, respectively ( $n = 12$ ;  $P = 0.5$ ). Ankle systolic blood pressure values at affected limb were  $84 \pm 13$  mm Hg before administration and were increased to  $94 \pm 11$  mm Hg on the 14th day of administration ( $n = 12$ ;  $P = 0.4$ ).

Pain was assessed with a numerical rating scale in six patients who complained of rest pain (Table 2). Rest pain disappeared in three of the six patients (patient 6, 4/0; patient 9, 4/0; and patient 13, 3/0, as before/after the administration of carperitide) and was reduced in another patient (no. 1, 3/1). In patient 4, although the pain once worsened in the

early phase of administration (from 4 to 6), the injections were continued, and the pain was reduced to level 1 within a week. In another patient (no. 5), the carperitide infusion was stopped at d 7 because rest pain had worsened (4 to 6) (Fig. 3A). All patients who felt the rating score of rest pain reduced could stop to use pain relievers or hypnotics.

Exercise performance was carried out on all patients with intermittent claudication except for those who could not walk as a result of rest pain or weakness (patients 2, 7, 8, 10, and 12) (Fig. 3C). The pain-free walking distance was assessed in four patients and prolonged in all of them after the carperitide administration (patient 2, 290 to 380 m; patient 7, 240 to 560 m; patient 8, 200 to 800 m; patient 10, 100 to 200 m). In another patient with a stair-climb test, the floor number of pain-free stair climbing was increased from five to seven.

Five patients had multiple foot ulcers, and dermatologists in our hospital had recommended foot amputation. Al-

**TABLE 3.** Changes in ABI by 14 d administration of carperitide

Patient no.	Systolic BP (mm Hg)				ABI	
	Brachial		Ankle		Before	2 wk
	Before	2 wk	Before	2 wk		
1	96	182	35	106	0.36	0.58
2	141	101	115	89	0.82	0.88
3	159	140	69	81	0.43	0.58
4	88	115	83	140	0.94	1.22
5	138	NA	86	NA	0.62	NA
6	176	151	188	154	1.07	1.02
7	150	123	112	108	0.75	0.88
8	113	117	97	78	0.86	0.67
9	162	100	0	0	0	0
10	101	99	60	90	0.59	0.91
11	143	161	66	111	0.46	0.69
12	153	132	80	83	0.52	0.63
13	201	164	107	91	0.53	0.55
Mean	140	132	84	94	0.61	0.72
(SEM)	10	8	13	11	0.08	0.09

Values of brachial and ankle brachial pressure and ABI in each patient before and on the d 14 of administration. The administration was interrupted on the d 7 in patient 5. Data of patient 5 are excluded for the calculation of mean and SEM. NA, Not assessed.

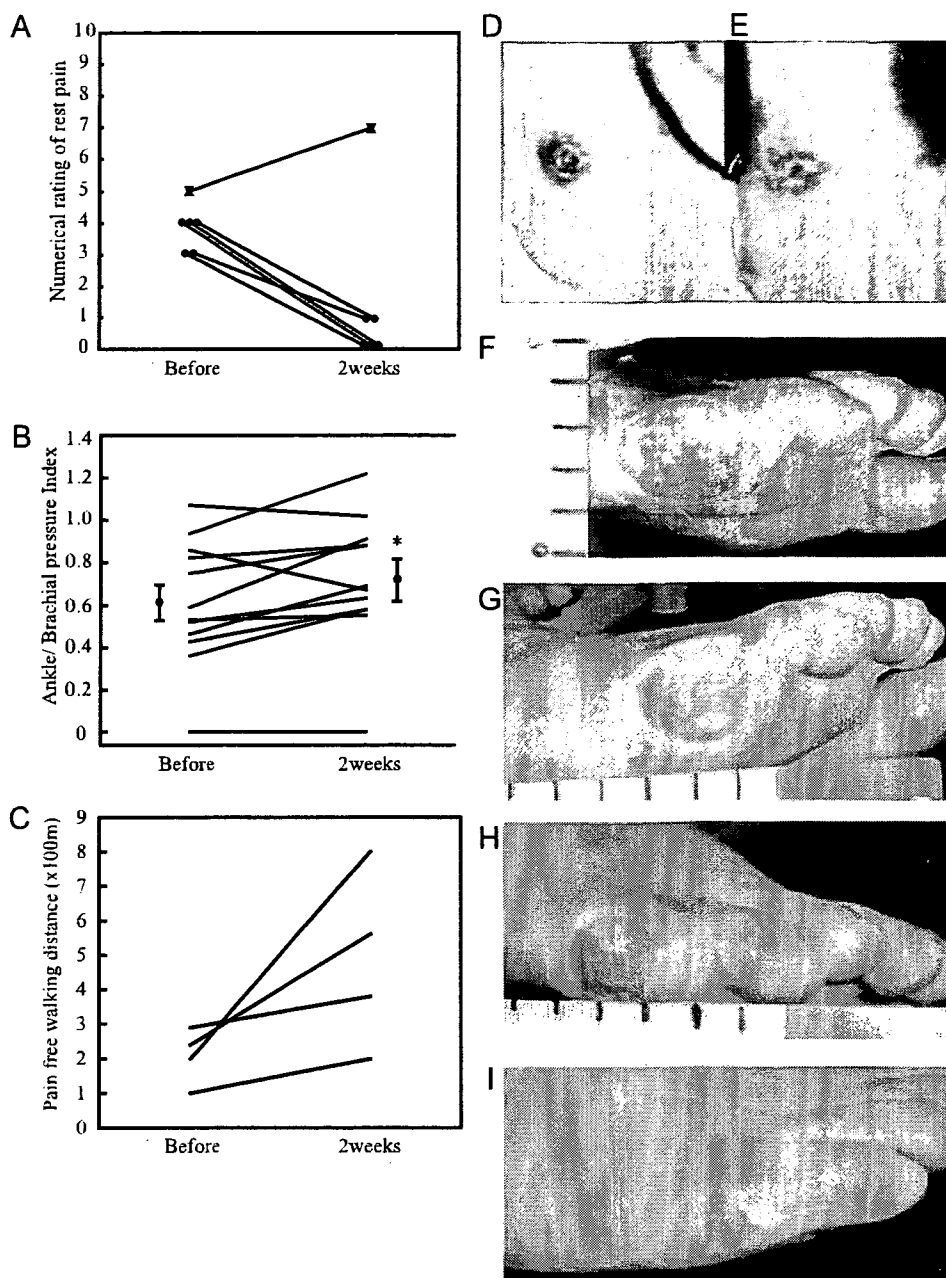


FIG. 3. Changes in symptoms resulting from carperitide infusion. A, Changes of 11-grade numerical rating of rest pain; B, changes in ABI of affected or worse side limb in each patient. Mean values are shown together with error bars (SEM) before and 2 wk after the carperitide administration.  $n = 12$ ;  $P < 0.05$ . The administration was interrupted on the seventh day in patient 5, and ABI was undetectable in the affected limb of patient 9. C, Change in exercise tolerance assessed by pain-free walking distance; D–I, improvement of foot ulcer in patients 4 and 13. Pictures are before (D) and after 8-wk administration of carperitide (E) in patient 4 and before (F) and after 3 (G) and 6 (H) wk administration of carperitide and 4 months after leaving hospital (I) in patient 13. Pitting foot edema was observed in patient 4 (E).

though the ulcers did not change in severity in two cases (patients 5 and 6), they improved in another three cases (patients 4, 11, and 13) for whom foot amputations could be avoided. A representative case is shown in Fig. 3, D–I.

Other changes observed during administration were as follows: hot sensation in lower extremities in eight patients (nos. 1, 2, 4, 5, 6, 7, 8, and 13), transient flush and slight nausea in one patient (no. 2), pitting edema in both feet in five patients on hemodialysis (nos. 1, 4, 6, 11, and 13), and an increase in menstrual bleeding in a patient (no. 2).

### Discussion

Diabetic foot is one of the most severe complications of diabetes mellitus and often results in leg amputation. Be-

cause it has been shown that an impairment of angiogenesis in patients with diabetes mellitus is a major cause of diabetic gangrene, we tried to generate a mouse model to investigate the mechanism of the impaired angiogenesis in diabetes. We induced diabetes in mice with STZ injections, and the mice were subjected to a femoral artery ligation after exposure to diabetic conditions (a blood glucose level higher than 220 mg/dl) for 4–26 wk. Although a 4-wk exposure to the diabetic condition did not affect blood flow recovery after the femoral artery ligation, exposure to high blood glucose for longer periods (16 or 26 wk) significantly impaired the blood flow recovery. This observation suggests that a quite long period of high blood glucose level is required to impair ischemia-induced collateral vessel formation. We therefore

selected 16 wk after the STZ induction of diabetes as the time point when the femoral artery ligation was performed on mice.

We showed here that carperitide, a recombinant human ANP, significantly accelerated blood flow recovery in a mouse model of ischemia-induced angiogenesis in both nondiabetic and diabetic conditions. The blood flow recovery in carperitide-treated diabetic mice was improved to a level similar to that in vehicle-treated nondiabetic mice. A histological analysis revealed that capillary density in the muscle of the ischemic limb was reduced in diabetic mice. The carperitide infusion significantly recovered capillary density in diabetic mice to the level in vehicle-treated nondiabetic mice. These observations indicate that carperitide can improve ischemia-induced angiogenesis, which accelerates blood flow recovery in diabetic conditions. We have shown that an increase of circulating BNP levels by targeted overexpression of the murine BNP gene in the liver or an overexpression of cGK throughout the body by the transgenic technology can accelerate the restoration of blood flow in limb ischemia experimentally generated by a femoral artery ligation, which results from the promotion of ischemia-induced angiogenesis through the activation of the ERK cascade (14). We have also shown that ANP at a physiological concentration induces proliferation and migration of ECs and enhances endothelial regeneration via activating ERK1/2 and phosphatidylinositol 3-kinase/Akt pathways in an *in vitro* wound healing assay using the cells from either coronary arteries or umbilical veins of humans (11). CNP, another member of the NP family, was shown to enhance migration of ECs and to accelerate reendothelialization in vein grafts after an arterial bypass surgery, although CNP inhibits proliferation and migration of vascular SMCs (16, 17). NPs use particulate GCs as their signaling receptors and share cGMP signaling pathways, especially signaling through cGKI, with NO, which activates soluble GC to generate cGMP (4). It is known that NO is a mediator of VEGF, which is a potent mitogen for vascular ECs and induces angiogenesis (19). A significant portion of VEGF-induced human EC proliferation is reportedly mediated by cGKI (20). In diabetes, hyperglycemia induces formation of reactive oxygen species, which decrease the bioavailability of NO (21). Taken together, deterioration of cGMP signaling appears to be a key process leading to the impaired angiogenesis and PAD in diabetes. In this study, the administration of carperitide could overcome the impairment of cGMP signaling in diabetic conditions, and it would be a new, therapeutic approach to PAD with diabetes. Because the urinary cGMP excretion rate is inversely correlated with the grade of Fontaine's classification in PAD patients (5), an impairment of cGMP signaling appears to be a common feature of PAD. We therefore investigated the therapeutic potential of carperitide administration in PAD patients.

We did not assign participants to a vehicle-treated group for an ethical reason; most cases of participants had been treated with conventional therapies, which had not accomplished appreciable effects. The carperitide administration significantly increased ABI, effectively relieved symptoms including intermittent claudication and rest pain, and promoted the healing of foot ulcers in PAD patients. The dosage

of carperitide we used in the human study was optimized for each patient according to the maximum permissible dosage, which is the highest dose possible without causing an excessive fall in systolic blood pressure, because sensitivity to exogenously administered ANP differs among patients depending, presumably, upon basal plasma ANP levels. Although doses of carperitide administration were lower than those usually given in the treatment of CHF, plasma cGMP levels were increased twice as much as basal levels, and relief from the characteristic signs and symptoms of PAD became possible. This observation suggests that a blood pressure fall would not limit the therapeutic use of carperitide for PAD patients.

It is reported that asymmetric dimethylarginine (ADMA), an endogenous inhibitor of endothelial NO synthase, is accumulated in patients with end-stage renal disease (ESRD) and a high plasma ADMA level is a strong indicator of risks for all-cause mortality and cardiovascular events (22). It might be speculated that responses to the carperitide administration are better in ESRD patients than in non-ESRD patients, because carperitide is supposed to restore cGMP signaling, which is impaired by ADMA, via an activation of GC-A. Considering heterogeneity of patients' clinical characteristics, a larger number of participants will be needed to address this issue.

All patients, for whom exercise tolerance was evaluated, had been treated with conventional therapies using per os and per cutaneous medications under hospitalization and been encouraged to walk for at least 3 wk without any increases of pain-free walking distances. A 2-wk carperitide administration was then added to the conventional therapies and resulted in significantly improved exercise tolerance. The improvement, therefore, cannot be explained by a training effect only.

NPs have various biological effects on vascular functions other than the promotion of angiogenesis, and some of them appear favorable to treating PAD. NPs regulate vascular tone, and CNP, especially, is a candidate for endothelial-derived hyperpolarizing factor, which plays a fundamental role in the regulation of local blood flow and systemic blood pressure (23). In the clinical investigation of this paper, changes in symptoms and ABI appeared within a few days or a week of the administration. The effect of carperitide on symptoms in the early phase might be due to a vasodilatory action of ANP to some extent, because the changes appeared too early to be regarded as effects of vascular regeneration. On the other hand, the elongation of pain-free walking distance persisted after the cessation of the administration was ceased, and ABI remained elevated for several months after the end of administration. If the vasodilatory action of ANP is the only mechanism of the improvement, the effects of carperitide should disappear promptly at the cessation of the infusion, because the half life of ANP in circulation is a couple of minutes (24).

In patients with advanced arteriosclerosis, severe calcification of arterial walls in lower extremities can cause an overestimation of ankle blood pressure. Where vasodilators such as carperitide were used in such patients, ABI might be increased solely due to a decrease in brachial blood pressure. In this study, we observed slight decreases in brachial blood

pressure, but we could observe increases in ankle blood pressure although the changes were not statistically significant. Increases in ABI, therefore, should not be false and should be, at least in part, the result of blood flow recovery.

The improvement in exercise tolerance and ABI might, therefore, be achieved by modifying vascular endothelial structure or promoting vascular regeneration. Plasma VEGF levels were not significantly elevated by the carperitide infusion in this study, indicating that VEGF is not an essential mediator of carperitide's effects on PAD symptoms. It is reported that NPs elicit antiinflammatory and antithrombotic effects in animals (17, 25, 26), and further investigation will be needed to see whether such effects of NPs are clinically significant.

Carperitide is often used to treat CHF patients in Japan, and its safety is clinically proven. No critical side effects were observed in this study. An increase in menstrual bleeding observed in a participant could be accidental or a result of ANP's vasodilatory action, because the symptom faded soon after the cessation of the infusion. There are, however, several reports indicating the physiological significance of CNP/GC-B signaling in the control of ovarian cycling (27, 28). A close observation would be needed where carperitide infusion would be applied to women of reproductive age for a long duration (more than 2 wk). Leg edema appeared in three patients, who were in relatively serious states of the foot disease. Many PAD patients develop postoperative edema after surgeries of revascularization (29), which indicates that they have circulatory inadequacy for autoregulating blood hydrostatic pressure. Because ANP reportedly plays an essential role in maintaining vascular permeability via GC-A on vascular ECs (30), edema might result from this direct action on vascular endothelium.

### Conclusion

This study revealed that a long-duration diabetic condition impaired ischemia-induced angiogenesis and blood flow recovery in a mouse model of hind-limb ischemia and that ANP as a therapeutic agent for CHF can restore the ischemia-induced angiogenesis in diabetic mice. Based on this observation, we applied carperitide administration to 13 PAD patients and found that carperitide infusion at doses lower than those for CHF could safely improve signs and symptoms. Carperitide administration, therefore, can be a new therapeutic strategy for PAD, and it appears effective in patients for whom conventional therapies do not work well.

### Acknowledgments

We thank our colleagues in Kyoto University Hospital for referring patients and assistance; the staff of the Institute of Laboratory Animals, Graduate School of Medicine, Kyoto University for animal care; Ms. Akane Nonoguchi for technical assistance; and Ms. Ayumi Ishida and Ms. Shihō Takada for secretarial assistance.

Received August 7, 2007. Accepted November 1, 2007.

Address all correspondence and requests for reprints to: Hiroshi Itoh, M.D., Ph.D., Department of Internal Medicine, Keio University School of Medicine, Shinanomachi, Shinjuku-ku, Tokyo 160-8582, Japan. E-mail: hiito@kuhp.kyoto-u.ac.jp.

This work was supported by the Kyoto University 21st Century Centers of Excellence Program "Integration of Transplantation Therapy

and Regenerative Medicine"; Grant-in-Aid for Scientific Research from the Ministry of Health, Labor, and Welfare; the Ministry of Education, Culture, Sports, Science, and Technology and the Japan Smoking Foundation; Grant of Regenerative Medicine Realization Project of the Ministry of Education, Culture, Sports, Science, and Technology; Fifth Grant for Clinical Vascular Function from the Kimura Memorial Heart Foundation; Grant from Takeda Medical Foundation; Grant from Japan Foundation of Applied Enzymology; and the Research Grant for Cardiovascular Disease 19C-7 from the Ministry of Health, Labor, and Welfare.

Disclosure Statement: The authors of this manuscript have nothing to declare.

### References

- Rivard A, Silver M, Chen D, Kearney M, Magner M, Annex B, Peters K, Isner JM 1999 Rescue of diabetes-related impairment of angiogenesis by intramuscular gene therapy with adeno-VEGF. *Am J Pathol* 154:355–363
- Martin A, Komada MR, Sane DC 2003 Abnormal angiogenesis in diabetes mellitus. *Med Res Rev* 23:117–145
- Tesfamariam B, Cohen RA 1992 Free radicals mediate endothelial cell dysfunction caused by elevated glucose. *Am J Physiol* 263:H321–H326
- Tamura N, Chrisman TD, Garbers DL 2001 The regulation and physiological roles of the guanylyl cyclase receptors. *Endocr J* 48:611–634
- Boger RH, Bode-Boger SM, Thiele W, Junker W, Alexander K, Frolich JC 1997 Biochemical evidence for impaired nitric oxide synthesis in patients with peripheral arterial occlusive disease. *Circulation* 95:2068–2074
- Sugawara A, Nakao K, Morii N, Yamada T, Itoh H, Shiono S, Saito Y, Mukoyama M, Arai H, Nishimura K, Obata K, Yasue H, Ban T, Imura H 1988 Synthesis of atrial natriuretic polypeptide in human failing hearts. Evidence for altered processing of atrial natriuretic polypeptide precursor and augmented synthesis of  $\beta$ -human ANP. *J Clin Invest* 81:1962–1970
- Mukoyama M, Nakao K, Hosoda K, Suga S, Saito Y, Ogawa Y, Shirakami G, Jougasaki M, Obata K, Yasue H, Kambayashi Y, Inoue K, Imura H 1991 Brain natriuretic peptide as a novel cardiac hormone in humans. Evidence for an exquisite dual natriuretic peptide system, atrial natriuretic peptide and brain natriuretic peptide. *J Clin Invest* 87:1402–1412
- Suga S, Nakao K, Hosoda K, Mukoyama M, Ogawa Y, Shirakami G, Arai H, Saito Y, Kambayashi Y, Inoue K 1992 Receptor selectivity of natriuretic peptide family, atrial natriuretic peptide, brain natriuretic peptide, and C-type natriuretic peptide. *Endocrinology* 130:229–239
- Colucci WS, Elkayam U, Horton DP, Abraham WT, Bourge RC, Johnson AD, Wagoner LE, Givertz MM, Liang CS, Neibaur M, Haight WH, Lejemtel TH 2000 Intravenous nesiritide, a natriuretic peptide, in the treatment of decompensated congestive heart failure. Nesiritide Study Group. *N Engl J Med* 343:246–253
- Suwa M, Seino Y, Nomachi Y, Matsuki S, Funahashi K 2005 Multicenter prospective investigation on efficacy and safety of carperitide for acute heart failure in the 'real world' of therapy. *Circ J* 69:283–290
- Kook H, Itoh H, Choi BS, Sawada N, Doi K, Hwang TJ, Kim KK, Arai H, Baik YH, Nakao K 2003 Physiological concentration of atrial natriuretic peptide induces endothelial regeneration in vitro. *Am J Physiol Heart Circ Physiol* 284:H1388–H1397
- Ogawa Y, Itoh H, Tamura N, Suga S, Yoshimasa T, Uehira M, Matsuda S, Shiono S, Nishimoto H, Nakao K 1994 Molecular cloning of the complementary DNA and gene that encode mouse brain natriuretic peptide and generation of transgenic mice that overexpress the brain natriuretic peptide gene. *J Clin Invest* 93:1911–1921
- Pfeifer A, Klatt P, Massberg S, Ny L, Sausbier M, Himeiss C, Wang GX, Korth M, Aszodi A, Andersson KE, Krombach F, Mayerhofer A, Ruth P, Fassler R, Hofmann F 1998 Defective smooth muscle regulation in cGMP kinase I-deficient mice. *EMBO J* 17:3045–3051
- Yamahara K, Itoh H, Chun TH, Ogawa Y, Yamashita J, Sawada N, Fukunaga Y, Sone M, Yurugi-Kobayashi T, Miyashita K, Tsujimoto H, Kook H, Feil R, Garbers DL, Hofmann F, Nakao K 2003 Significance and therapeutic potential of the natriuretic peptides/cGMP/cGMP-dependent protein kinase pathway in vascular regeneration. *Proc Natl Acad Sci USA* 100:3404–3409
- Suga S, Nakao K, Itoh H, Komatsu Y, Ogawa Y, Hama N, Imura H 1992 Endothelial production of C-type natriuretic peptide and its marked augmentation by transforming growth factor- $\beta$ . Possible existence of "vascular natriuretic peptide system". *J Clin Invest* 90:1145–1149
- Doi K, Ikeda T, Itoh H, Ueyama K, Hosoda K, Ogawa Y, Yamashita J, Chun TH, Inoue M, Masatsugu K, Sawada N, Fukunaga Y, Saito T, Sone M, Yamahara K, Kook H, Komeda M, Ueda M, Nakao K 2001 C-type natriuretic peptide induces redifferentiation of vascular smooth muscle cells with accelerated reendothelialization. *Arterioscler Thromb Vasc Biol* 21:930–936
- Ohno N, Itoh H, Ikeda T, Ueyama K, Yamahara K, Doi K, Yamashita J, Inoue M, Masatsugu K, Sawada N, Fukunaga Y, Sakaguchi S, Sone M, Yurugi T, Kook H, Komeda M, Nakao K 2002 Accelerated reendothelialization with suppressed thrombogenic property and neointimal hyperplasia of rabbit jugular vein grafts by adenovirus-mediated gene transfer of C-type natriuretic peptide. *Circulation* 105:1623–1626

18. Naruko T, Ueda M, van der Wal AC, van der Loos CM, Itoh H, Nakao K, Becker AE 1996 C-type natriuretic peptide in human coronary atherosclerotic lesions. *Circulation* 94:3103–3108
19. Morbidelli L, Chang CH, Douglas JG, Granger HJ, Ledda F, Ziche M 1996 Nitric oxide mediates mitogenic effect of VEGF on coronary venular endothelium. *Am J Physiol* 270:H411–H415
20. Hood J, Granger HJ 1998 Protein kinase G mediates vascular endothelial growth factor-induced Raf-1 activation and proliferation in human endothelial cells. *J Biol Chem* 273:23504–23508
21. Ceriello A, Motz E 2004 Is oxidative stress the pathogenic mechanism underlying insulin resistance, diabetes, and cardiovascular disease? The common soil hypothesis revisited. *Arterioscler Thromb Vasc Biol* 24:816–823
22. Kielstein JT, Zoccali C 2005 Asymmetric dimethylarginine: a cardiovascular risk factor and a uremic toxin coming of age? *Am J Kidney Dis* 46:186–202
23. Chauhan SD, Nilsson H, Ahluwalia A, Hobbs AJ 2003 Release of C-type natriuretic peptide accounts for the biological activity of endothelium-derived hyperpolarizing factor. *Proc Natl Acad Sci USA* 100:1426–1431
24. Ingwersen SH, Jorgensen PN, Eiskjaer H, Johansen NL, Madsen K, Faarup P 1992 Superiority of sandwich ELISA over competitive RIA for the estimation of ANP-270, an analogue of human atrial natriuretic factor. *J Immunol Methods* 149:237–246
25. Kiemer AK, Vollmar AM 2001 The atrial natriuretic peptide regulates the production of inflammatory mediators in macrophages. *Ann Rheum Dis* 60(Suppl 3):68–70
26. Scotland RS, Cohen M, Foster P, Lovell M, Mathur A, Ahluwalia A, Hobbs AJ 2005 C-type natriuretic peptide inhibits leukocyte recruitment and platelet-leukocyte interactions via suppression of P-selectin expression. *Proc Natl Acad Sci USA* 102:14452–14457
27. Tamura N, Doolittle LK, Hammer RE, Shelton JM, Richardson JA, Garbers DL 2004 Critical roles of the guanylyl cyclase B receptor in endochondral ossification and development of female reproductive organs. *Proc Natl Acad Sci USA* 101:17300–17305
28. Acuff CG, Huang H, Steinhilber ME 1997 Estradiol induces C-type natriuretic peptide gene expression in mouse uterus. *Am J Physiol* 273:H2672–2677
29. Coats P, Wadsworth R 2005 Marriage of resistance and conduit arteries breeds critical limb ischemia. *Am J Physiol Heart Circ Physiol* 288:H1044–H1050
30. Sabrane K, Kruse MN, Fabritz L, Zetsche B, Mitko D, Skryabin BV, Zwiener M, Baba HA, Yanagisawa M, Kuhn M 2005 Vascular endothelium is critically involved in the hypotensive and hypovolemic actions of atrial natriuretic peptide. *J Clin Invest* 115:1666–1674

*Endocrinology* is published monthly by The Endocrine Society (<http://www.endo-society.org>), the foremost professional society serving the endocrine community.

---

**2nd Annual International Adrenal Cancer Symposium:  
Clinical and Basic Science  
March 14-15, 2008  
18 AMA PRA Category I Credits**

Sponsored by the University of Michigan Comprehensive Cancer Center Multidisciplinary Adrenal Cancer Program, the 2nd Annual International Adrenal Cancer Symposium will be an exciting combination of science, clinical care and resources for the physician and patient. The conference will cover all aspects of the study of adrenal cancer and the treatment of patients with the disease. Internationally renowned speakers from 14 countries will participate in oral and poster sessions that will cover epidemiology, pathogenesis, genetics, cancer stem cells, historic and emerging therapies, mouse models of adrenal cancer, new developments in tumor profiling, worldwide collaborative groups and tumor registries, together with resources for the practitioner and community of adrenal cancer scientists.

For More Information:

Registrar

Office of Continuing Medical Education

University of Michigan Medical School

G1200 Towsley Center

1500 E. Medical Center Drive, SPC 5201

Ann Arbor, MI 48109-5201

Phone: 734-763-1400; Fax: 734-936-1641

<http://www.med.umich.edu/intmed/endocrinology/acs.htm>

<http://cme.med.umich.edu/>



# Augmentation of Neovascularization in Hindlimb Ischemia by Combined Transplantation of Human Embryonic Stem Cells-Derived Endothelial and Mural Cells

Kenichi Yamahara<sup>1,3</sup>, Masakatsu Sone<sup>1,3</sup>, Hiroshi Itoh<sup>1,2\*</sup>, Jun K. Yamashita<sup>3</sup>, Takami Yurugi-Kobayashi<sup>3</sup>, Koichiro Homma<sup>2</sup>, Ting-Hsing Chao<sup>4</sup>, Kazutoshi Miyashita<sup>1,2</sup>, Kwijun Park<sup>1</sup>, Naofumi Oyamada<sup>1</sup>, Naoya Sawada<sup>1</sup>, Daisuke Taura<sup>1</sup>, Yasutomo Fukunaga<sup>1</sup>, Naohisa Tamura<sup>1</sup>, Kazuwa Nakao<sup>1</sup>

**1** Department of Medicine and Clinical Science, Kyoto University Graduate School of Medicine, Kyoto, Japan, **2** Department of Internal Medicine, Keio University School of Medicine, Tokyo, Japan, **3** Laboratory of Stem Cell Differentiation, Stem Cell Research Center, Institute for Frontier Medical Science, Kyoto University, Kyoto, Japan, **4** Division of Cardiology, Department of Internal Medicine, National Cheng Kung University Medical Center, Tainan, Taiwan

## Abstract

**Background:** We demonstrated that mouse embryonic stem (ES) cells-derived vascular endothelial growth factor receptor-2 (VEGF-R2) positive cells could differentiate into both endothelial cells (EC) and mural cells (MC), and termed them as vascular progenitor cells (VPC). Recently, we have established a method to expand monkey and human ES cells-derived VPC with the proper differentiation stage in a large quantity. Here we investigated the therapeutic potential of human VPC-derived EC and MC for vascular regeneration.

**Methods and Results:** After the expansion of human VPC-derived vascular cells, we transplanted these cells to nude mice with hindlimb ischemia. The blood flow recovery and capillary density in ischemic hindlimbs were significantly improved in human VPC-derived EC-transplanted mice, compared to human peripheral and umbilical cord blood-derived endothelial progenitor cells (pEPC and uEPC) transplanted mice. The combined transplantation of human VPC-derived EC and MC synergistically improved blood flow of ischemic hindlimbs remarkably, compared to the single cell transplantations. Transplanted VPC-derived vascular cells were effectively incorporated into host circulating vessels as EC and MC to maintain long-term vascular integrity.

**Conclusions:** Our findings suggest that the combined transplantation of human ES cells-derived EC and MC can be used as a new promising strategy for therapeutic vascular regeneration in patients with tissue ischemia.

**Citation:** Yamahara K, Sone M, Itoh H, Yamashita JK, Yurugi-Kobayashi T, et al (2008) Augmentation of Neovascularization in Hindlimb Ischemia by Combined Transplantation of Human Embryonic Stem Cells-Derived Endothelial and Mural Cells. PLoS ONE 3(2): e1666. doi:10.1371/journal.pone.0001666

**Editor:** Tailoi Chan-Ling, University of Sydney, Australia

**Received:** November 5, 2007; **Accepted:** January 24, 2008; **Published:** February 27, 2008

**Copyright:** © 2008 Yamahara et al. This is an open-access article distributed under the terms of the Creative Commons Attribution License, which permits unrestricted use, distribution, and reproduction in any medium, provided the original author and source are credited.

**Funding:** This work is supported by a grant-in-aid for scientific research (the Japanese Ministry of Education, Culture, Sports, Science and Technology), a research grant from them 21st COE Program for Integration of Transplantation Therapy and Regenerative Medicine (Japan Society for the Promotion of Science), a research grant from the Project for Development of Regenerative Medicine (the Japanese Ministry of Education, Culture, Sports, Science and Technology), and a research grant from the Japan Foundation for Aging and Health (the Japanese Ministry of Health, Labor and Welfare).

**Competing Interests:** The authors have declared that no competing interests exist.

\*E-mail: hrith@scitc.keio.ac.jp

\*These authors contributed equally to this work.

## Introduction

Embryonic stem (ES) cells, with their extensive regeneration potential and functional multilineage differentiation capacity, are now highlighted as promising cell sources for regenerative medicine. Previously we reported that mouse ES cells-derived vascular endothelial growth factor receptor-2 (VEGFR2) positive cells could differentiate into both endothelial cells (EC) and mural cells (MC) (pericytes and vascular smooth muscle cells) and reproduce the vascular organization process, which we termed "vascular progenitor cells (VPC)" [1]. Transplanted VPC into tumor-bearing nude mice were incorporated into blood vessels and

significantly increased blood flow, which suggests that VPC might be useful for augmenting vessel growth in ischemic tissue [2].

We have demonstrated that human as well as monkey ES cells possessed different differentiation kinetics of VPC derived from mouse ES cells [3,4]. In contrast to mouse ES cells, undifferentiated human ES cells already expressed VEGFR2. After the induction of differentiation on OP9 feeder cells, VEGFR2 positive and tumor rejection antigen-1 (TRA1: a marker indicative of undifferentiated cell phenotype) negative cells appeared at day 8. We confirmed that VEGFR2 positive cells at this stage effectively differentiated into both VE-cadherin positive EC and  $\alpha$ -smooth muscle actin ( $\alpha$ SMA) positive MC to suffice as human VPC.

Human VPC-derived VEGFR2<sup>+</sup> VE-cadherin<sup>+</sup> cells, which were considered as EC at an early differentiation stage, formed a network structure on Matrigel-coated dishes.

Based upon these works, in the present study we transplanted human VPC-derived vascular cells; that is, EC and MC in a murine hindlimb ischemia model. By transplantation of these EC and MC differentiated from human VPC, we investigated whether and how they could be incorporated as EC and MC into the sites of neovascularization, compared to human peripheral blood and umbilical cord blood-derived endothelial progenitor cell (EPC) transplantation [5–7]. Furthermore, we specifically asked whether the combined transplantation of human VPC-derived EC and MC could induce stable vascular regeneration to achieve long-term vascular integrity.

## Results

### Characterization of Transplanted Human VPC-derived Vascular Cells

Flow cytometric analysis disclosed that 20–40% of expanded human VPC-derived EC retained the expression of the endothelial cell-related markers, including VE-cadherin, VEGFR2, CD34, CD31 and CD105, and all of the cells were negative for a panleukocyte marker CD45, monocyte/macrophage marker (CD11b), and stem/progenitor markers (AC133 and c-kit) (Figure 1a). By the double immunostaining of CD31 and  $\alpha$ SMA, the cells negative for CD31 were exclusively positive for  $\alpha$ SMA (Figure 1b), but weak or negative for staining with other MC markers, including calponin, smooth muscle myosin heavy chain 1 (SM1) and 2 (SM2) (data not shown).

Immunocytochemistry of expanded human VPC-derived MC revealed that all these cells were positive for  $\alpha$ SMA, calponin, SM1 and SM2 (Figure 1c). Analysis by reverse transcription-polymerase chain reaction (RT-PCR) also confirmed that mRNA expressions of these MC markers were upregulated in human VPC-derived MC and negative in sorted VE-cadherin<sup>+</sup> fraction of expanded human VPC-derived EC (Figure 1d). Although cultured human aortic smooth muscle cells (hAoSMC) expressed a high level of h-caldesmon, its expression in human VPC-derived MC was not detected. Furthermore, mRNA for skeletal (myogenin and MyoD) or cardiac (cardiac troponin T (cTnT) and I (cTnI)) specific marker was not detected in human VPC-derived MC (Figure 1e).

### Characterization of Transplanted Human EPC

Flow cytometric analysis of pEPC demonstrated that these cells mainly exhibited two light-scattering properties: one was consistent with a relatively large cell size (gate P1) and the other was found in a smaller gate P2 (Figure 2a). The P1-gated cells were positive for DiI-acLDL uptake and ulex-lectin binding (Figure 2b), and exhibited the reported EPC phenotype [6,8]. However, the smaller P2-gated cells were low positive for DiI-acLDL/ulex-lectin (Figure 2c). Therefore, we performed subsequent fluorescence activated cell sorter (FACS) analysis of pEPC on the P1-gated cells.

As shown in Figure 2d, nearly all pEPC expressed the hematopoietic markers CD45 (99.9%) and CD54 (99.9%) and the monocyte/macrophage markers CD14 (99.0%), CD11b (98.7%), and CD11c (98.9%). The monocyte/macrophage or endothelial markers CD31 (58.3%) and CD105 (70.1%) were also expressed. A much lower percentage of these cells expressed the endothelial cell-related markers VE-cadherin (1.6%), VEGFR2 (5.4%), and von Willebrand Factor (vWF) (0.3%), or the stem/progenitor cell markers AC133 (1.0%), c-kit (0.4%), and CD34 (0.2%).

Flow cytometric analysis of magnetic cell separation system (MACS)-sorted uEPC showed more than 80% of these cells were

positive for CD34 (data not shown). Similar to pEPC, almost all CD34<sup>+</sup> fraction of uEPC expressed the hematopoietic markers CD45 (99.0%) and CD54 (84.9%) (Figure 2e). However, the expression of monocyte/macrophage markers was limited in uEPC (CD14 5.7%, CD11b 99.7%, CD11c 21.3%), and significant number of these cells was positive for the endothelial cell-related markers, including VE-cadherin (11.2%), VEGFR2 (8.1%), and vWF (7.9%). In addition, these CD34<sup>+</sup> uEPC expressed the stem/progenitor markers AC133 (80.6%) and c-kit (95.3%).

### Long-term Improvement of Blood Flow of Ischemic Hindlimb by Human VPC-derived Vascular Cell Transplantation

To examine the comparative effectiveness of transplanted human VPC-derived vascular cells for vascular regeneration, we set up six groups as follows (Figure 3);

- 1) EC+MC group (n=9): the mixture of  $0.5 \times 10^6$  human VPC-derived EC and  $0.5 \times 10^6$  MC, with the total cell number of  $1 \times 10^6$ ,
- 2) EC group (n=20):  $0.5 \times 10^6$  human VPC-derived EC,
- 3) MC group (n=18):  $0.5 \times 10^6$  human VPC-derived MC,
- 4) uEPC group (n=10):  $1 \times 10^6$  umbilical cord-derived CD34<sup>+</sup> cells,
- 5) pEPC group (n=16):  $1 \times 10^6$  peripheral mononuclear cells (MNC)-derived EPC,
- 6) Control group (n=17): only 100  $\mu$ l PBS.

To analyze subcutaneous hindlimb perfusion, laser Doppler perfusion image (LDPI) analysis was performed (Figure 4a). Throughout the 42 day follow-up period, significantly accelerated limb perfusion improvement was observed in the VPC-derived EC+MC-transplanted group, compared to the EPC and control groups (Figure 4b,  $P < 0.001$  vs. control, pEPC, uEPC, and MC groups,  $P = 0.002$  vs. EC group, repeated measures ANOVA followed by Bonferroni's multiple comparison test).

At day 14, blood flow of the mice transplanted with EPC (the ratio of ischemic/non-ischemic blood flow:  $0.907 \pm 0.058$  in pEPC and  $0.942 \pm 0.075$  in uEPC) ( $P = 0.035$  and  $0.028$ , compared to the control group), as well as MC ( $0.957 \pm 0.056$ ) ( $P = 0.006$ ) and EC ( $0.901 \pm 0.063$ ) ( $P = 0.032$ ) showed significant increase, compared to the control group ( $0.730 \pm 0.042$ ) (Figure 4b). In the EC+MC group, the ratio of ischemic/non-ischemic blood flow markedly elevated to  $1.187 \pm 0.083$  ( $P < 0.0001$ ), compared to other groups.

Blood flow in the pEPC group, however, did not increase thereafter and no significant difference in the blood flow between the pEPC and control group was seen at days 28 and 42 (Figure 4b). In the uEPC group, significant blood flow recovery was seen at day 42 ( $0.990 \pm 0.054$ ) ( $P = 0.009$ ), compared to the control group ( $0.749 \pm 0.039$ ). The blood flow in the VPC-derived vascular cells-transplanted groups progressively increased. At day 42, the calculated perfusion ratio of ischemic to non-ischemic hindlimb significantly elevated to  $0.943 \pm 0.057$  for the MC ( $P = 0.013$ ),  $1.038 \pm 0.059$  for the EC ( $P = 0.0002$ ), and  $1.231 \pm 0.067$  for the EC+MC group ( $P < 0.0001$ ) compared to the control group ( $0.749 \pm 0.039$ ). Between the cell mixture transplantation (EC+MC) group and the single cell transplantation (EC or MC) groups, the blood flow of ischemic hindlimbs was significantly different at day 42 ( $P < 0.05$ ).

### Effective Contribution of Human VPC-derived Vascular Cells for Vascular Regeneration

Fixed tissues harvested from ischemic hindlimbs at day 7 were inspected by the fluorescence stereomicroscope (Leica, Wetzlar,

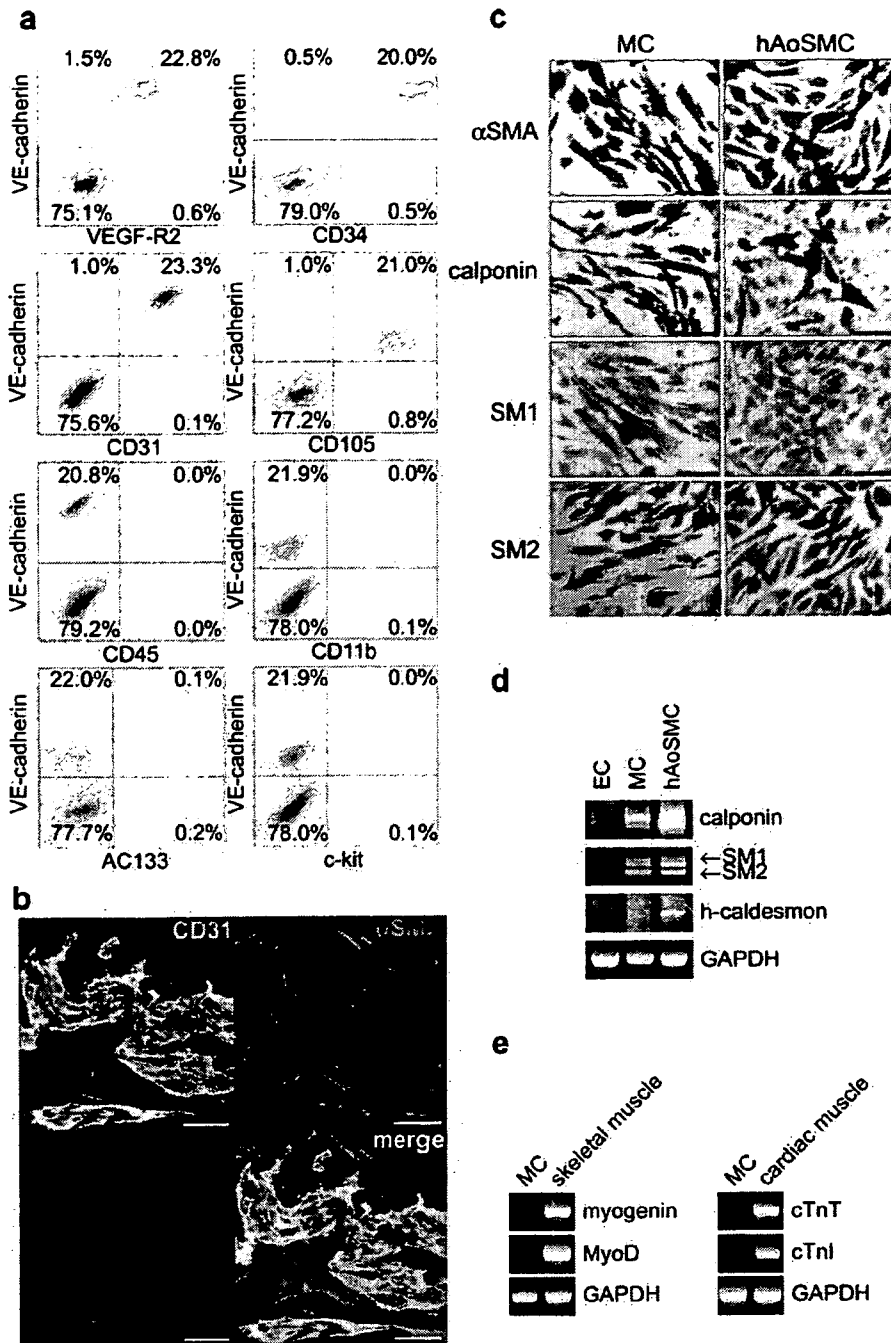


**Figure 1. Characterization of transplanted human VPC-derived vascular cells.** a) Flow cytometric analysis of cell surface markers on expanded human VPC-derived VEGF-R2<sup>+</sup>VE-cadherin<sup>+</sup> cells (=EC). b) Immunofluorescence image of CD31 (green) and  $\alpha$ SMA (red) with nuclear staining (blue) in expanded EC. Scale bar: 100  $\mu$ m. c) Immunostaining of mural cell markers (brown) with hematoxyline counter-staining of expanded VPC-derived VEGF-R2<sup>+</sup>VE-cadherin<sup>+</sup> cells (=MC). Scale bar: 100  $\mu$ m. d, e) RT-PCR analysis of mural cell (d) and skeletal/cardiac specific (e) markers in human VPC-derived vascular cells. doi:10.1371/journal.pone.0001666.g001

Germany). Extended distribution of DiI-positive transplanted cells was clearly seen in both VPC-derived EC+MC and pEPC-transplanted hindlimbs (Figure 5a). We also detected some DiI-positive vessel-like formation in the lung and spleen, but no obvious tumor-like structures were seen (data not shown).

Ischemic hindlimbs at day 14 were sectioned and treated with streptavidin conjugated dye to stain intravenously injected biotinylated isolectin B<sub>4</sub>, followed by anti-human CD31 antibody, and scanned for the incorporation of transplanted cells into circulating vessels. In the EC+MC group, we found that human

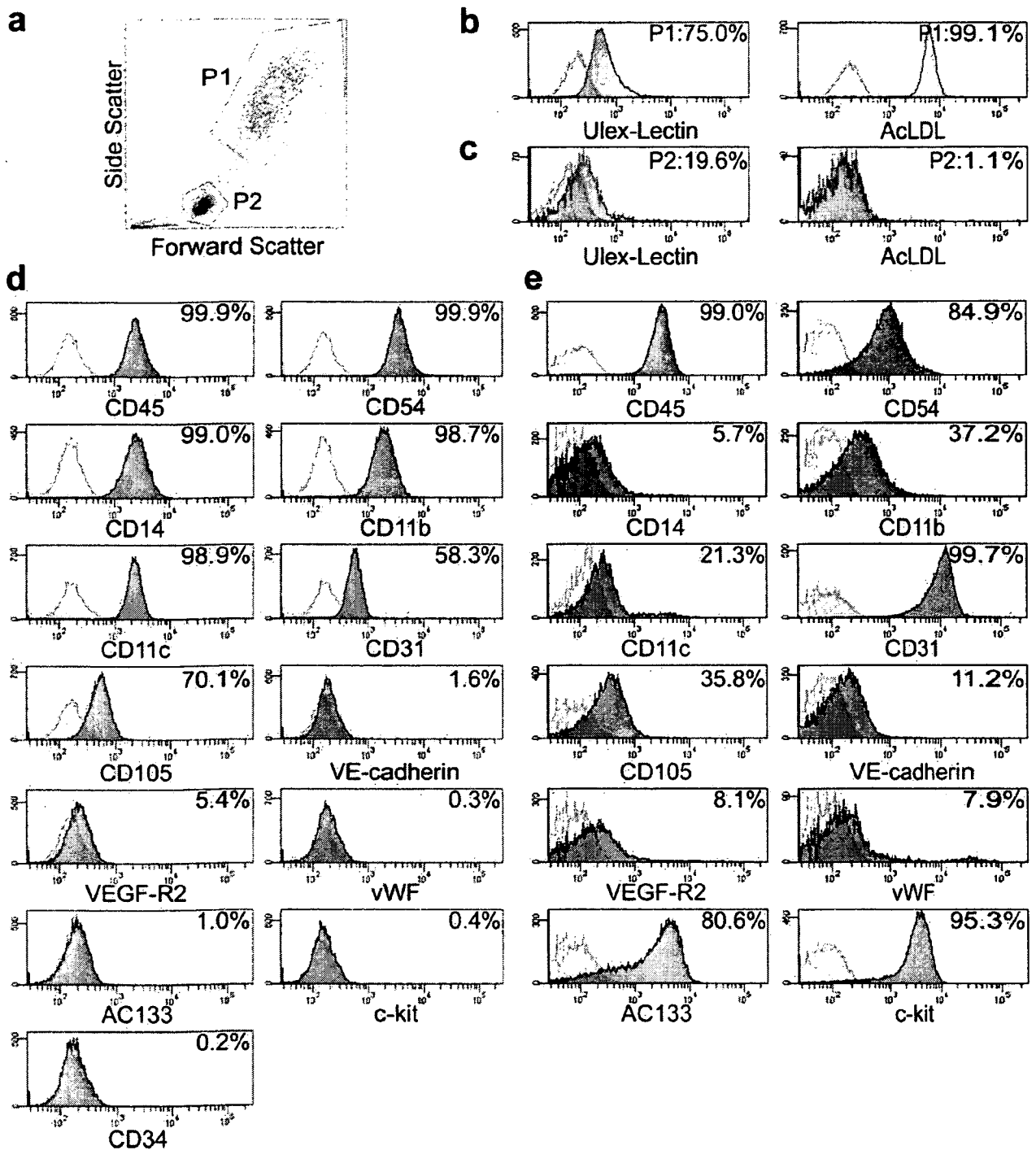


**Figure 2. Characterization of peripheral blood and umbilical cord-derived EPC (pEPC and uEPC, respectively) by flow cytometer.** a) Representative forward and side scatter profile of cultured pEPC. b-d) Flow cytometric analysis of ulex-lectin binding/acLDL uptake (b, c) and various cell surface markers (d) in pEPC. e) Flow cytometric analysis of cell surface markers in uEPC.  
doi:10.1371/journal.pone.0001666.g002

CD31 positive cells formed capillaries with host EC, which were stained with isolectin B<sub>4</sub> (Figure 5b: arrowhead). Furthermore, some human CD31 positive cells solely formed capillary vessel (Figure 5b: arrow), which might indicate de novo vessel

formation from human VPC-derived EC. We also detected human CD31 positive cells in the pEPC and uEPC group; however, many of these cells were located within the lumen of host capillaries (Figure 5c, arrow).